Naval Research Laboratory
Washington, DC 20375-5000

NRL/MR/5313—92-7111

Extension of Fresnel Near-Field Region by Single-Cycle Sinusoidal Pulses

S.N. SAMADDAR

Radar Analysis Branch
Radar Division

August 21, 1992

Approved for public release; distribution unlimited.

REPORT DOCUMENTATION PAGE

Form Approved
OMB No. 0704-0188

1. AGENCY USE ONLY (Leave Blank)	2. REPORT DATE	3. REPORT TYPE AND DATES COVERED
	August 21, 1992	Interim

4. TITLE AND SUBTITLE

Extension of Fresnel Near-Field Region by Single-Cycle Sinusoidal Pulses

5. FUNDING NUMBERS

PE - 62111N
DN - 020-051

6. AUTHOR(S)

S.N. Samaddar

7. PERFORMING ORGANIZATION NAME(S) and ADDRESS(ES)

Naval Research Laboratory
Washington, DC 20375-5320

8. PERFORMING ORGANIZATION REPORT NUMBER

NRL/MR/5313—92-7111

9. SPONSORING/MONITORING AGENCY NAME(S) AND ADDRESS(ES)

Office of Naval Technology
Arlington, Virginia 22217-5000

10. SPONSORING/MONITORING AGENCY REPORT NUMBER

11. SUPPLEMENTARY NOTES

12a. DISTRIBUTION/AVAILABILITY STATEMENT

Approved for public release; distribution unlimited

12b. DISTRIBUTION CODE

13. ABSTRACT (Maximum 200 words)

A circular conducting disk antenna is excited by three uniform current waveforms, namely, a very high frequency CW $\sin\omega_0 t$, a single-cycle $\sin\omega_0 t$, and a single-cycle $\cos\omega_0 t$. The energy per cycle associated with each of these waveform is taken to be the same. From the behavior of the radiated energy densities along the axis of the disk, it is found that if the CW waveform extends the near field to unit distance, then the corresponding distances are 1.375 and 3.75 for the single-cycle $\sin\omega_0 t$ and the single-cycle $\cos\omega_0 t$, respectively. These results show that the method of energy transfer to a large distance along the axis of an aperture (or disk) becomes more efficient when a short pulse, instead of a CW source, is applied. This will have applications wherever a transmission of high intensity beam of energy far away from a radiating device is needed.

14. SUBJECT TERMS

Fresnel Region Single-cycle Sinusoidal Pulses
Electromagnetic Missiles Directed Short-Pulse
Near-Field
Fresnel Zone

15. NUMBER OF PAGES

57

16. PRICE CODE

17. SECURITY CLASSIFICATION OF REPORT	18. SECURITY CLASSIFICATION OF THIS PAGE	19. SECURITY CLASSIFICATION OF ABSTRACT	20. LIMITATION OF ABSTRACT
UNCLASSIFIED	UNCLASSIFIED	UNCLASSIFIED	SAR

CONTENTS

1. INTRODUCTION 1

2. DISCUSSIONS OF NUMERICAL RESULTS 3

3. CONCLUSIONS 7

4. ACKNOWLEDGEMENT 8

APPENDIX A 9

APPENDIX B 29

REFERENCES 43

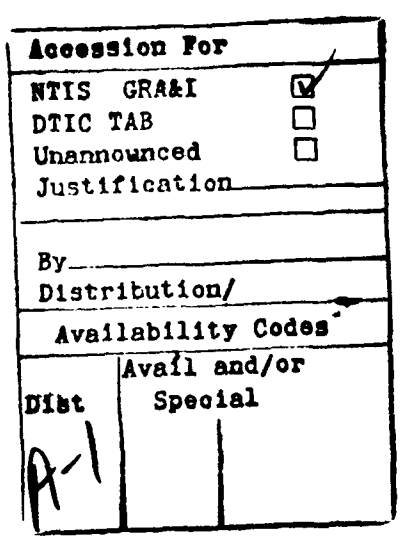

EXTENSION OF FRESNEL NEAR-FIELD REGION BY SINGLE-CYCLE SINUSOIDAL PULSES

1. INTRODUCTION

The theory of diffraction of a monochromatic (or a CW) wave [1,2] by a circular disk (or aperture) of radius $a = D/2$, shows that the diffracted energy density in the Fresnel near-field region decreases slower than $1/z^2$ on the axis of the disk. Beyond this region the well-known behavior is $1/z^2$ in the Fraunhofer region (far field region). Though there is no well-defined demarcation between the Fresnel and the Fraunhofer region, the optical [1,2] and the acoustical [3] literatures take this to be a^2/λ, where λ is the wavelength of the wave concerned. On the otherhand, it is a common practice in the antenna literature [4] to assume this boundary to lie between D^2/λ $(= 4a^2/\lambda)$ and $2D^2/\lambda$ $(= 8a^2/\lambda)$. An approximate theory [1] can be used to explain that as the point of observation z from the disk (or aperture) is made longer than a^2/λ, there is less than one Fresnel zone in the disk and the intensity of the wave energy decays as $1/z^2$ (as in the Fraunhofer region or far field). On the otherhand, as z is made to shrink towards the aperture along its axis, so that more than one Fresnel zone in the aperture contributes to the intensity at z, the energy density oscillates between zero and a maximum value. For extremely small z, this approximate theory is not applicable. The first maximum intensity appears at $z = a^2/\lambda$, beyond which the wave intensity starts to decrease like $1/z^2$. This observation then indicates that the Fresnel near-field region, where the energy density drops slower than $1/z^2$, increases as the frequency of the incident field increases. The decrease of intensity slower than $1/z^2$ implies also that the diffracted or radiated field is collimated.

In many applications which require transmission of high field intensity (such as an extended radar system), to a relatively long distance (a few hundred to a few thousand kilometers), in principle this distance can be made to fall within the Fresnel near-field region by simply increasing the frequency of the field as well as the aperture dimension of the radiator. However, just increasing the frequency of the monochromatic source of the radiator may not be an efficient method, as indicated in the following recent works [5,6,7,8].

Manuscript approved July 18, 1992.

Wu [5] who introduced the concept of "electromagnetic missile", defining the electromagnetic energy which decays slower than $1/r^2$, showed that some pulsed sources backed by a reflector can transmit electromagnetic energy to a great distance, where the field energy falls slower than the inverse of the square of the distance. Wu and Shen [6] also preformed an experiment in a laboratory for demonstrating the validity of the theory. Besides them, Ziolkowski and his associates [7,8] also investigated the behavior of a special type of highly collimated wave, named "localized wave transmission" which also required an excitation of an aperture by suitably created pulses. They [8] also conducted an acoustic experiment for verifying their concept and theory. The aims of these two groups ([5,6], [7,8]) appear to be the same, though their respective theoretical approaches and concepts are different. For instance, in the study of "electromagnetic missiles," a conventional method of solution of wave equation in the Fresnel region is needed, which makes it easier to understand the process of radiation. However, a special solution (appears to be unconventional) together with the choice of a special type of pulsed sources are required in Ziolkowski's is work. In spite of the apparent conceptual and methodological differences, the studies of both the "electromagnetic missiles" and the "localized wave transmission" show that directed short pulses encompassing a wide band of high frequencies are required. The results of these studies provide a clue to the question of finding a method of extending the Fresnel near-field region more efficiently.

In references [5,6] non-sinusoidal pulses with suitable forms were used so that the results could be expressed and interpreted conveniently. For non-sinusoidal pulses there is no unique and apparent equivalent wavelength, corresponding to which a Fresnel region can be identified. As a result, there is no convenient and well accepted way to determine the enhancement of the near-field region, when the source of radiation is a non-sinusoidal pulse. On the otherhand, for a sinusoidal pulse, such as a single-cycle $\sin\omega_0 t$ or $\cos\omega_0 t$, the extension of the Fresnel region can be ascertained in a convenient manner by comparing the respective results with those of a CW $\sin\omega_0 t$ source.

In view of the above observations, the present investigation, resembling the study of "electromagnetic missiles," studies the feasibility of extending the Fresnel near-field region of a conducting circular disk antenna [Fig. 1] excited by sinusoidal pulses, single-cycle $\sin\omega_0 t$ and single-cycle $\cos\omega_0 t$, which are more familiar. It may not be too difficult to generate a short pulse containing a few cycles of $\sin\omega_0 t$. The consideration of a single-cycle $\cos\omega_0 t$ appears to be more academic than realistic, nevertheless the results shed some light, pointing out clearly that the shorter the rise time of a pulse, the slower is the decay of the radiated energy density. The efficacy of a single-cycle $\sin\omega_0 t$ pulse over the corresponding CW $\sin\omega_0 t$ as exciting sources in extending the Fresnel near-field region (and hence collimating the radiated energy) lies in the cohesive contributions of all the higher frequencies equal to and above ω_0 (i.e. all ω in $\omega \geq \omega_0$) contained in the pulse.

In section 2 presentation and discussion of numerical results are made, followed by conclusions in section 3. Development of the theory of radiation in the Fresnel near-field region of a circular conducting disk excited by uniform sinusoidal current pulses and the associate analyses can be found in Appendixes A and B.

2. DISCUSSIONS OF NUMERICAL RESULTS

Since the behavior of the energy density as a function of the coordinate z along the axis of the conducting disk or the dimensionless distance $\alpha(=z/(D^2/\lambda_0))$ will demonstrate whether these sinusoidal pulses do indeed enhance the Fresnel near-field region, we shall first present the energy densities for different parameters. The wavelength λ_0 is defined by $\lambda_0 = 2\pi c/\omega_0$, where c is the velocity of light in free space. In Fig. 3a three normalized energy density expressions associated with a CW $\sin\omega_0 t$ current (Eq. 24, Appendix A), a single-cycle $\sin\omega_0 t$ pulse (Eq. 34a, Appendix A) and a single-cycle $\cos\omega_0 t$ (Eq. 34b, Appendix A) are presented as functions of α along the axis of the disk. The energy per cycle of each of these excitations is the same.

The behavior of the radiated normalized energy density, $P_{cw}/P_0 = \sin^2\left[\frac{\pi}{8\alpha}\right]$, corresponding to the CW $\sin\omega_0 t$ current source is well-known [3,5,6]. It is highly oscillatory for $\alpha \leq 1/8$, reaches the maximum value 1 at $\alpha = 1/4$, and then begins to drop monotonically. This oscillatory behavior of P_{cw} for $\alpha < 1/8$ is due to the fact that more than one Fresnel zone in the disk (source region) contributes to the illumination and causes interference. Here we make a distinction between the Fresnel zone and the Fresnel region. The Fresnel zone is located in the source region, whereas the Fresnel region lies in front of the radiator, where near-field radiation takes place.

In contrast the normalized radiated energy density P_s/P_0, associated with the single-cycle of $\sin\omega_0 t$, has a constant value unity without showing any oscillatory behavior in the region $\alpha \leq 1/8$. For $\alpha > 1/8$, it increases to a maximum value of 1.5 at $\alpha = 1/4$, from there it decreases monotonically with the increase of α. The oscillatory behavior of P_{cw} for $\alpha < 1/8$ is also absent in P_c/P_0, the normalized energy density corresponding to the single-cycle $\cos\omega_0 t$ excitation. This observation suggests that if there are nulls in the radiation pattern of a radiator excited by a monochromatic signal, those nulls can be eliminated by choosing a short pulse, the spectrum of which contains that monochromatic source frequency as a source of excitation.

However, the behavior of P_c/P_0 shows a peculiarity, since it begins to drop from unity to a minimum value (about 0.78) near $\alpha \simeq 0.162$, from where it starts to increase to a maximum value (about 1.58) at $\alpha \simeq 0.3$. Before attaining this maximum value P_c/P_0 passes through the point of maximum of P_s/P_0 at $\alpha = 1/4$. From $\alpha \simeq 0.3$, P_c/P_0 begins to decrease monotonically with α. although at a slower rate than either P_s/P_0 or P_{cw}/P_0, exhibiting the fact that P_c has a larger value than that of P_s or P_{cw}. Between $\alpha = 1/8$ and $1/4$, P_c is smaller than P_s. However, both P_s and P_c are larger everywhere than P_{cw}, if we agree that the average value of P_{cw}/P_0 is only 1/2 for $\alpha \leq 1/8$, since both P_s/P_0 and P_c/P_0 are unity. Although some graphs are shown for $\alpha = 0$ (or $z = 0$), they are not valid. However, α can be very small, depending on the value of λ_0 and the condition $a/z << 1$.

The larger values of P_s and P_c are due to the simultaneous and collective contributions of all the high frequencies exceeding ω_0 ($\omega \geq \omega_0$) contained in the single-cycle pulses. It is not, however, clear why P_c/P_0 is smaller than P_s/P_0 in the region $1/8 < \alpha < 1/4$. It may be that for a certain large ω_m the amplitudes of the frequency spectrum between $\omega_0 \leq \omega \leq \omega_m$ of the single-cycle $\cos\omega_0 t$ are smaller than those for the single-cycle $\sin \omega_0 t$, although the single-cycle $\cos \omega_0 t$ contains more high frequencies with large amplitudes in general. Note that the spectra of the single-cycle $\sin \omega_0 t$ and the single-cycle $\cos \omega_0 t$ behave like $1/\omega^2$ and $1/\omega$, respectively, as $\omega \to \infty$.

Figure 3a shows the behavior of P_{cw}, P_s and P_c for small values of $\alpha(\leq 1)$. On the other hand, Fig. 3b displays how P_{cw}, P_s and P_c decrease for larger values of α, which is helpful in determining whether P_s and P_c have indeed shown extension of the near-field region when compared with P_{cw}. For this purpose let us choose first a value of α, which we take to be 2 (i.e. $z = 2D^2/\lambda_0$) for convenience. At this distance along the axis of the disk P_{cw}/P_0 has a value about 0.03806, which is equivalent to -14.2 dB. We now find from Fig. 3b that P_s/P_0 and P_c/P_0 drop to this value at $\alpha = 11$ and 30 respectively. This finding can be interpreted as follows: when compared with a CW $\sin \omega_0 t$ excitation, the single-cycle $\sin \omega_0 t$ and the single-cycle $\cos \omega_0 t$ enhance the Fresnel near-field region by 37.5% and 275%, respectively. Although an ideal single-cycle $\cos\omega_0 t$ is not realizable (similar to the case of an ideal rectangular pulse, which is used in many examples in the literature for the purpose of illustrations) the associated results shed light in showing clearly that the higher the rate of rise of an exciting pulse, the slower is the decay of the radiated energy.

Let us now turn our attention for a moment to an interesting aspect of the initial time variation of a pulse and the corresponding behavior of its spectrum at high frequencies. Reference [6] shows that if the current pulse behaves like $t^{\epsilon - 1/2}$ for small values of t, then its spectrum $\hat{F}(\omega)$ at high frequencies decreases like $\omega^{-(\epsilon + 1/2)}$. Consequently, the corresponding radiated energy density $P(z)$ along the axis of the disk drops as $z^{-2\epsilon}$ with increasing z. In order for a current pulse to produce a

"missile" effect, they required $0 < \epsilon < 1$, so that the energy density decreases slower than $1/z^2$. For a single-cycle $\sin\omega_0 t$ we can not apply these results in a strict sense. For instance, for small t, $\sin\omega_0 t$ increases as t. If we use their results, we get $\epsilon = 3/2$, showing $\hat{F}_s(\omega) \sim 1/\omega^2$ and $P_s/P_0 \sim 1/z^3$, without displaying any "missile" effect. Although the behavior of $\hat{F}_s(\omega)$ is correct as $\omega \to \infty$, our result [Eq. 34a, Appendix A] shows that $P_s(z)/P_0$ behaves like $1/z^2$ for very large z. In spite of this behavior of $P_s(z)$, it displays [Figs. 3a and 3b] effective enhancement of the near-field, i.e. showing "missile" effect. Using a similar argument for the single-cycle $\cos\omega_0 t$, one finds that for small t, $\cos\omega_0 t = 1$ indicating $\epsilon = 1/2$, $\hat{F}_c(\omega) \sim 1/\omega$ and $P_c \sim 1/z$ for large z. Surprisingly, such behaviors agree with our results, although the single-cycle $\cos\omega_0 t$ is unrealizable.

The above discussions pertain to the axial behavior of the energy densities, which are not too difficult to compute. On the other hand, the off-axis (i.e. $s = \rho/a > 0$) behavior of either P_s or P_c is very difficult to compute, since the expressions (32a) and (32b) of Appendix A converge slowly. In $s = \rho/a$, ρ is the perpendicular distance from the z-axis. However, for $s = 1$ and $s >> 1$, it is relatively easy to calculate P_s and P_c in closed form [Eqs. (39a) to 40b, Appendix A]. For $s >> 1$ the associated infinite series can be adequately approximated by retaining only the first term. In Figs. (4a) and (4b) we show these results. Figure 4a displays the behavior of the normalized energy density P_s/P_0 for $s = 0$, 0.125, 0.25 and 1. Similarly, Fig. 4b presents P_c/P_0 for the same values of s. The cases, $s = 0.125$ and 0.25 for P_s/P_0 are computed by using Eqs. (36a) and (36b) of Appendix A, respectively. For $s >> 1$, both normalized energy densities become so small, that they are excluded from these displays. In general these results show that both P_s and P_c are concentrated in the vicinity of the disk axis and drop rapidly with increasing values of s. Such behaviors of P_s and P_c, together with an examination of the expressions (24) to (27) of Appendix A, indicate that the radiated energy density associated with a short-pulse excitation is highly focused towards the axis of symmetry of the radiator and extends to a larger distance along this axis when compared to the corresponding results for the CW excitation.

In Figs. 5a through 5d the behavior of the normalized radiated electric field, E_{xs}, associated with the single-cycle $\sin\omega_0 t$ are presented. The corresponding behaviors of E_{xc} (not shown) associated with the single-cycle $\cos\omega_0 t$ can be obtained by taking the first derivative of E_{xs} with respect to $\omega_0 t^*$, ($t^* = t - z/c$). Figures 5a through 5d show E_{xs} as a function of the normalized time $\tau = t/T$, where $T = 2\pi/\omega_0$ is the period of one cycle, for $s = 0$ and 1 at a given distance α, parallel to the z-axis. The thick dotted curve is common to both $s = 0$ and 1. It follows from Eq. 28a of Appendix A that for $s = 0$, the two signals, one radiated from the center of the disk [the first term of (28a)] and those radiated from the circumference of the disk (second term), overlap for $\alpha < 1/8$. For $s = 1$ [Eq. 30a, Appendix A], the radiated fields from these two regions overlap for $\alpha > 1$, otherwise they are separated. Thus, Figs. 5a through 5c show that these two radiated signals overlap for $s = 0$, and are well separated for $s = 1$. However, in Fig. 5b one finds that for $s = 1$, the two signals begin to combine. The second signal ($s = 1$), which comes from the center as well as from other circumferential points that are farther away, is much smaller than the first signal, which comes only from the nearest point on the circumference. The interference of these rays among themselves reduces the amplitude of the second signal. Figure 5d shows that for a large $s(=5)$, the off-axis field strength is very small, which agrees with what is intuitively expected.

3. CONCLUSIONS

It has been shown that in order to extend the Fresnel's near field region, which process being the same as collimating (or focusing) the radiated energy, infront of a conducting circular disk antenna, a single-cycle $\sin\omega_0 t$ current pulse is more efficient than the corresponding CW $\sin\omega_0 t$ current source. Such an ability of a single-cycle pulse lies in the cohesive contributions of the high frequencies above ω_0 ($\omega \geq \omega_0$) contained in the pulse. Assuming that the near field region extends to unit distance (along the disk axis) due to the excitation by a CW $\sin\omega_0 t$ current, it is found that the corresponding distances are 1.375 and 3.75 when the exciting current sources are a single-cycle

$\sin\omega_0 t$ and a single-cycle $\cos\omega_0 t$, respectively. The use the single-cycle $\cos\omega_0 t$ pulse may be regarded as more academic than realistic, nevertheless the corresponding results show clearly that the shorter the rise time of a pulse consisting of large amplitudes of high frequency components, the slower is the rate of fall of the radiating energy, thereby proving itself more efficient in focusing or collimating the field energy in the vicinity of the axis of symmetry of the radiator. If there is a way to generate a short pulse, the frequency spectrum of which falls like $1/\omega^{\beta}$ as ω increases indefinitely, with β lying at least in the range $1 \leq \beta < 2$, it should be welcomed as a potential candidate for the applications where the above mentioned behavior of the radiated energy in the Fresnel region is desirable.

The results of this study indicate also that if there are nulls in the radiation pattern of a radiating system excited by a monochromatic signal, those nulls can be made to disappear if, instead, a short pulse, the spectrum of which contains that frequency of the monochromatic source, is used.

4. ACKNOWLEDGEMENT

The importance of the topic of this study was suggested by Dr. M.I. Skolnik, with whom the author had many useful discussions. The author appreciates also very much the generous assistance provided by Mr. C.E. Fox, Jr., Mr. M.W. Kim and Dr. E.L. Mokole in obtaining numerical results.

APPENDIX A

I. GENERAL FORMULATION

For the transmission of a directed and collimated electromagnetic energy one needs a focusing device in addition to an antenna. However, for the purpose of demonstration and simplicity we shall take a perfectly conducting circular disk of radius a as an antenna, which also serves as a focusing mechanism. This circular disk antenna is excited by sinusoidal single-cycle uniform current pulses, $\sin\omega_0 t$ and $\cos\omega_0 t$, respectively. The primary reason of our choice of these sinusoidal pulses is to show, by comparing with the result corresponding to a cw sinusoidal excitation, whether these pulses do indeed extend the Fresnel's near field region.

At first, the problem will be formulated in the frequency domain, and then the corresponding time domain result will be obtained by an application of the inverse Fourier transform. It should be noted that the assumption of exciting the circular disk by a uniform current imposes an unnecessary restriction, which implies filtering out very high frequencies. Nevertheless, it is adequate [5,6] for the purpose at hand. Consider a thin perfectly conducting disk of radius a, lying in the x-y plane in otherwise free space [Fig. 1]. The center of the disk coincides with the origin of the coordinate system. This disk antenna is excited by a uniform x-directed surface current $\hat{J}_x(\vec{r}',\omega)$, where $\vec{r}'$ is on the disk and $\omega = 2\pi f$ is the angular frequency, which will excite all the rectangular components of the electromagnetic field except H_x. The non-zero field components can be expressed in terms of the x-directed vector potential $\hat{A}_x(\vec{r},\omega)$. Since we are interested in the transmission or radiation of electromagnetic energy in the z direction only, which is perpendicular to the circular disk, only the components E_x and H_y contribute. The x-component of the vector potential in the frequency domain is given by

$$\hat{A}_x(\vec{r},\omega) = (\mu_0/4\pi)\iint \hat{J}_x(\vec{r}',\omega)\,(e^{ikR}/R)\,dS' \qquad (1)$$

The integration is over the surface of the disk, where $R = |\vec{r} - \vec{r'}|$, $k = \omega/c = 2\pi/\lambda$ and $\vec{r}(x,y,z)$ and $\vec{r'}(x',y',0)$ are the observation and source coordinates, respectively. In the Fresnel region, where $a/\lambda >> 1$ and $z/a >> 1$, the R in the exponential is approximated by [3-6].

$$R = |\vec{r} - \vec{r'}| \simeq z + (x - x')^2/2z + (y - y')^2/2z \tag{2a}$$

$$= z + (\rho^2 + \rho'^2)/2z - (\rho\rho'/z)\cos(\phi - \phi')\Big\}$$

where

$$x = \rho\cos\phi,\ y = \rho\sin\phi \tag{2b}$$

$$x' = \rho'\cos\phi' \text{ and } y' = \rho'\sin\phi'$$

and $\rho/z << 1$, $a/z << 1$. In the denominator of the integrand in (1), R is approximated by z. The approximations indicated by (2a) and (2b) with $a/\lambda > > 1$ imply that the Fresnel region confines itself close to the axis of the circular disk. For a uniform current let us write

$$\hat{J}_x(\vec{r'},\omega) = I_0\,\hat{F}(\omega), \tag{3}$$

The constant I_0 has a dimension ampere/meter. Then using (2a) and (2b) in (1), we have

$$\hat{A}_x(\vec{r},\omega) = \left[I_0\,\mu_0\,\hat{F}(\omega)/(4\pi z)\right]\int_0^a d\rho'\rho'\,e^{ik\rho'^2/2z}\int_0^{2\pi} e^{-i(k\,\rho\rho'/z)\cos(\phi - \phi')}\,d\phi'. \tag{4}$$

The integral over ϕ' is $2\pi J_0(k\,\rho\rho'/z)$, where $J_0(x)$ is a Bessel function of order zero. Introducing now the following change of variables

$$\zeta = \rho'/a,\ u = k\,\rho a/z, \text{ and } \gamma = ka^2/z, \tag{5}$$

the expression (4) can be re-expressed as

$$\hat{A}_x(\vec{r},\omega) = \left[I_0\,\mu_0\,\hat{F}(\omega)/(2z)\right]\exp\left[ik(z + \rho^2/2z)\right] I(\gamma,u), \tag{6a}$$

where

$$I(\gamma,u) = a^2\int_0^1 J_0(u\,\zeta)\exp(i\gamma\,\zeta^2/2)\,\zeta\,d\zeta. \tag{6b}$$

The integral $I(\gamma,u)$ in (6b) cannot be evaluated in closed form. However, it can be expressed in terms of two Lommel's functions, $U_1(\gamma,u)$ and $U_2(\gamma,u)$ [9, 10, 11] in the following manner

$$I(\gamma,u) = (zc/\omega)\, e^{i\gamma/2}\, [U_1(\gamma,u) - i\, U_2\,(\gamma,u)], \tag{7a}$$

where

$$U_1\,(\gamma,u) = \gamma \int_0^1 J_0\,(u\,\zeta) \cos\{\gamma(1-\zeta^2)/2\}\,\zeta\, d\zeta, \tag{7b}$$

$$= \sum_{m=0}^{\infty} (-1)^m\, (\gamma/u)^{2m+1}\, J_{2m+1}(u).$$

and

$$U_2(\gamma,u) = \gamma \int_0^1 J_0\,(u\zeta) \sin\{\gamma(1-\zeta^2)/2\}\,\zeta d\zeta \tag{7c}$$

$$= \sum_{m=0}^{\infty} (-1)^m\, (\gamma/u)^{2m+2}\, J_{2m+2}(u).$$

The representation of $I(\gamma,u)$ given by (7a)-(7c), although valid for all $s = \rho/a = u/\gamma$, is suited more for large s. For example, when $s >> 1$, only the $m = 0$ term is sufficient to obtain an accurate approximation of $I(\gamma,u)$, i.e., $I(\gamma,u) \simeq (zc/\omega)U_1(\gamma,u)\exp(i\gamma/2) \simeq (zc/\omega)\cdot \exp(i\gamma/2)J_1\,(u)/s + O\,(1/s^2)$. An alternative representation of $I(\gamma,u)$, which is suited for small values of s, can be presented as follows [11]. Note that the notations used here are different from those in [11]. Define first

$$C(\gamma,u)/2 = \int_0^1 J_0(u\zeta) \cos(\gamma\,\zeta^2/2)\,\zeta d\zeta, \tag{8a}$$

$$S(\gamma,u)/2 = \int_0^1 J_0(u\zeta) \sin(\gamma\,\zeta^2/2)\,\zeta d\zeta, \tag{8b}$$

$$V_0(s,u) = \sum_{m=0}^{\infty} (-1)^m\, s^{2m}\, J_{2m}(u), \tag{9a}$$

$$V_1\,(s,u) = \sum_{m=0}^{\infty} (-1)^m\, s^{2m+1}\, J_{2m+1}(u). \tag{9b}$$

Then we have

$$I(\gamma,u)/a^2 = C(\gamma,u)/2 + iS(\gamma,u)/2 \tag{10}$$

$$C(\gamma,u) = (2/\gamma)\,[\sin(u^2/2\gamma) + V_0(s,u)\sin(\gamma/2) - V_1(s,u)\cos(\gamma/2)], \tag{11a}$$

$$S(\gamma,u) = (2/\gamma)\,[\cos(u^2/2\gamma) - V_0(s,u)\cos(\gamma/2) - V_1(s,u)\sin(\gamma/2)]. \tag{11b}$$

The field components $\hat{E}_x(\vec{r},\omega)$ and $\hat{H}_y(\vec{r},\omega)$ can be obtained using the following relations in the Fresnel region.

$$\hat{E}_x(\vec{r},\omega) = i\omega\,[\hat{A}_x + (1/k^2)\frac{\partial^2}{\partial x^2}\hat{A}_x] \simeq i\omega\,\hat{A}_x(\vec{r},\omega), \tag{12a}$$

$$\hat{H}_y(\vec{r},\omega) = (1/\mu_0)\frac{\partial}{\partial z}\hat{A}_x \simeq (i\omega/\eta_0)\,\hat{A}_x(\vec{r},\omega), \tag{12b}$$

where $\eta_0 = \sqrt{\mu_0/\epsilon_0}$. The time-dependent radiated electric field in the Fresnel region is then given by the following Fourier transform.

$$E_x(\vec{r},t) = (1/2\pi)\int_{-\infty}^{\infty}\hat{E}_x(\vec{r},\omega)\,e^{-i\omega t}\,d\omega$$

$$= (i/2\pi)\,\mu_0 I_0 \int_{-\infty}^{\infty} I(\gamma,u)\,[\omega\hat{F}(\omega)/(2z)]\exp\left[-i\omega\{t - \left[z + \frac{\rho^2}{2z}\right]/c\}\right]d\omega \tag{13}$$

The other quantity of interest is the z-directed energy density at a point in the Fresnel region and expressed as

$$P(\vec{r}) = \int_{-\infty}^{\infty}\vec{E}(\vec{r},t)\times\vec{H}(\vec{r},t)\cdot\hat{z}\,dt$$

$$= (1/2\pi)\int_{-\infty}^{\infty}\hat{E}_x(\vec{r},\omega)\,\hat{H}_y^{*}(\vec{r},\omega)\,d\omega$$

$$= [I_0^2\,\eta_0/(8\pi)]\int_{-\infty}^{\infty}|\hat{F}(\omega)|^2\,(\frac{\omega}{cz})^2\,|I(\gamma,u)|^2\,d\omega, \tag{14}$$

where

$$|I(\gamma,u)|^2 = (cz/\omega)^2\,[U_1^2(\gamma,u) + U_2^2(\gamma,u)], \tag{15a}$$

which is suitable for $\rho/a = s > 1$ and

$$|I(\gamma,u)|^2 = (a^2/\gamma)^2\,[1 + V_0^2(s,u) + V_1^2(s,u) - 2V_0(s,u)\cos\{(\gamma + u^2/\gamma)/2\} - 2V_1(s,u)\sin\{(\gamma + u^2/\gamma)/2\}], \tag{15b}$$

which is suited for $s < 1$.

Except for $s = 0$ and $s = 1$, none of the above integrals, (13) and (14), can be evaluated in closed forms. However, for small values of s, $|I(\gamma,u)|^2$ given by (15b) can be used in a series form in powers of s. On the otherhand, for large values of s Eq. (15a) can be used to expressing it as a series in powers of (1/s). Similar statement holds for the expression of the electric field (13). Let us now express $I(\gamma,u)$ for various values of s, namely, $s = 0,1$, $s << 1$ and $s >> 1$. These will be found to be very useful in evaluating $E_x(\vec{r},t)$ and $P(\vec{r})$. For $s = 0$, it is easier to compute $I(\gamma,u)$ from (6b), although (7) and (10) may also be used. Thus for $s = 0$ we have

$$I(\gamma,u)|_{s=0} = 2(cz/\omega)\sin\left[\frac{\omega a^2}{4cz}\right]\exp\left[\frac{ia^2\omega}{4cz}\right], \tag{16a}$$

$$|I(\gamma,u)|_{s=0}|^2 = 4(cz/\omega)^2\sin^2\left[\frac{\omega a^2}{4cz}\right], \tag{16b}$$

For $s << 1$ using (9), (10), and (11) one finds

$$I(\gamma,u)/a^2 \simeq (i/\gamma)\left[\exp\left[-i\,\frac{k^2 a^2 s^2}{2z}\right] - \exp\left[\frac{ik^2 a^2}{2z}\right]\left\{J_0(u) + isJ_1(u) - s^2 J_2(u) + O(s^3)\right\}\right] \tag{17a}$$

where

$$u = ka^2 s/z.$$

Note that for very small s, $J_0(u) \simeq 1$, $J_1(u) = O(s)$ and $J_2(u) = O(s^2)$.

$$|I(\gamma,u)|^2 \simeq (z/k)^2 \left[1 + J_0^2(u) - 2\cos(ka^2/2z)J_0(u) - 2s\sin(ka^2/2z)J_1(u)\right.$$

$$\left. + s^2\left\{J_1^2(u) - 2J_0(u)J_2(u) + 2\cos(ka^2/2z)J_2(u)\right\} + \cdots\right]$$

$$s << 1. \tag{17b}$$

The expressions (17a) and (17b) reduce to (16a) and (16b) respectively for $s = 0$. For $s = 1$ either (7) or (10) may be used and the results are

$$I(\gamma,u)_{s=1} = I(\gamma,\gamma) = i(zc/\omega)\exp(i\gamma/2)\left[e^{-i\gamma} - J_0(\gamma)\right]/2, \tag{18a}$$

and

$$|I(\gamma,\gamma)|^2 = (cz/\omega)^2\,[1 + J_0^2(\gamma) - 2J_0(\gamma)\cos\gamma]/4. \tag{18b}$$

For very large values of s, the representations (7) and (15a) are appropriate. Thus we have for $s >> 1$

$$I(\gamma,u) \simeq (zc/\omega)\exp(i\gamma/2)\,[J_1(u)/s - iJ_2(u)/s^2 + O(1/s^3)], \tag{19a}$$

and

$$|I(\gamma,u)|^2 \simeq (zc/\omega)^2 J_1^2(u)/s^2,\ s >> 1. \tag{19b}$$

II. BEHAVIOR OF FIELD AND ENERGY DENSITY IN THE FRESNEL REGION DUE TO EXCITATION BY SINUSOIDAL PULSES

In this study we shall consider only two sinusoidal current pulses, namely single-cycle $\sin\omega_0 t$ and $\cos\omega_0 t$, where ω_0 is the angular carrier frequency. The respective spectra of these pulses are

$$\hat{F}_s(\omega) = -\omega_0\,(1 - \exp(i\omega T))/(\omega^2 - \omega_0^2), \tag{20a}$$

for the sine pulse and

$$\hat{F}_c(\omega) = i\omega(1 - \exp(i\omega T))/(\omega^2 - \omega_0^2), \tag{20b}$$

for the cosine pulse, where $T = 2\pi/\omega_0$. As the frequency ω increases indefinitely, one finds

$$|\hat{F}_s(\omega)| = O(1/\omega^2) \tag{21a}$$

and

$$|\hat{F}_c(\omega)| = O(1/\omega). \tag{21b}$$

For single-cycle pulses $\sin\omega_0 t$ and $\cos\omega_o t$, $\hat{F}(\omega)$ in (13) and (14) are replaced by $\hat{F}_s(\omega)$ and $\hat{F}_c(\omega)$, respectively.

Since we wish to compare the energy densities of the radiated fields associated with these single-cycle pulses at a given point in the Fresnel region with that of a CW sinusoidal signal ($\sin\omega_0 t$ or $\cos\omega_0 t$), it is necessary to normalize the energy content of these signals. Therefore, we shall assume that the energy of each of the single-cycle sinusoidal pulses is the same as the energy per cycle of the corresponding CW signal. This assumption then leads to the following expression for the square of the magnitude of the spectrum of a CW sinusoidal ($\sin\omega_0 t$ or $\cos\omega_0 t$) signal.

$$|\hat{F}_{cw}(\omega)|^2 = (\pi^2/(2\omega_0))\,[\delta(\omega - \omega_0) + \delta(\omega + \omega_0)]. \tag{22}$$

where δ is the Dirac's delta function. Replacing $|\hat{F}(\omega)|^2$ in (14) by $|\hat{F}_{cw}(\omega)|$, the energy density of the sinusoidal CW excitation can be expressed as

$$P_{cw}(\bar{r}) = P_0\,(\omega_0/(2cz))^2\,|I(\gamma,u)|_{\omega=\omega_0}|^2, \tag{23}$$

where $P_0 = (I_0^2\eta_0/2)(\pi/\omega_0)$ is a constant, which has a dimension of Watts-sec per meter. It may be noted that $|I(\gamma,u)|^2$ is an even function of ω.

For $s = 0$, using (16b) in (23), the energy density along the axis of the circular disk due to a CW sinusoidal excitation is given by the well-known expression [3,5].

$$P_{cw}(\bar{r})|_{s=0} = P_{cw}(z) = P_0 \sin^2\left[\frac{\pi}{8\alpha}\right] \tag{24}$$

where $\alpha = z/(4a^2/\lambda_0)$ is a normalized distance along the axis of the circular disk and $\lambda_0 = 2\pi c/\omega_0$. Next from (17b) and (23) we have for $s << 1$

$$P_{cw}(\bar{r}) \simeq (P_0/4)\,[1 + J_0^2\left(\frac{\pi s}{2\alpha}\right) - 2J_0\left(\frac{\pi s}{2\alpha}\right)\cos\left(\frac{\pi}{4\alpha}\right) - 2sJ_1\left(\frac{\pi s}{4\alpha}\right)\sin\left(\frac{\pi}{4\alpha}\right)$$

$$+ s^2\left\{J_1^2\left(\frac{\pi s}{2\alpha}\right) - 2J_0\left(\frac{\pi s}{2\alpha}\right)J_2\left(\frac{\pi s}{2\alpha}\right) + 2J_2\left(\frac{\pi s}{2\alpha}\right)\cos\left(\frac{\pi}{4\alpha}\right)\right\} + \cdots], \tag{25}$$

which reduces to Eq. (24) when $s = 0$.

For $s = 1$, one obtains from (18b) and (23)

$$P_{cw}(\bar{r}) = (P_0/16)[1 + J_0^2\left(\frac{\pi}{2\alpha}\right) - 2J_0\left(\frac{\pi}{2\alpha}\right)\cos\left(\frac{\pi}{2\alpha}\right) \tag{26}$$

Finally, for $s >> 1$ me have from (19b) and (23)

$$P_{cw}(\bar{r}) \simeq (P_0/4)\,J_1^2\left(\frac{\pi s}{2\alpha}\right)/s^2. \tag{27}$$

Before we proceed to compute the energy density integral (14) for the sinusoidal pulses let us now calculate the time dependent electric field, for both the pulses at various values of s. For this purpose the expression (13) will be evaluated using (7), (10), (16a) and (18a). The integration technique needed for the evaluation of (13) is discussed in the Appendix B. Here we shall simply present the pertinent results. On the axis ($s = 0$), the fields $E_{xs}(z,t)$ and $E_{xc}(z,t)$, excited by the single-cycle sine and cosine pulses, respectively are

$$E_{xs}(z,t) = E_0\left[-\sin\omega_0 t^*\,\{U(t^*) - U(t^* - T)\}\right.$$

$$\left. + \sin\omega_0(t^* - \frac{a^2}{2cz})\{U(t^* - \frac{a^2}{2cz}) - U(t^* - \frac{a^2}{2cz} - T)\}\right] \tag{28a}$$

$$E_{xc}(z,t) = E_0\left[-\cos\omega_0 t^*\,\{U(t^*) - U(t^* - T)\}\right.$$

$$\left. + \cos\omega_0\,(t^* - \frac{a^2}{2cz})\cdot\{U(t^* - \frac{a^2}{2cz}) - U(t^* - \frac{a^2}{2cz} - T)\}\right], \tag{28b}$$

where $E_0 = I_0\,\eta_0/2$ is a constant, which has a dimension of electric field, $t^* = t - z/c$ and $U(t)$ is

the unit step function. Note that (28b) can be obtained from (28a) by differentiating $E_{xs}(z,t)$ with respect to $\omega_0 t^*$. This should be expected, since E_{xs} and E_{xc} are excited by single-cycle $\sin\omega_0 t$ and $\cos\omega_0 t$, respectively. The first term of each of the expressions (28a) and (28b) is radiated directly from the center of the disk, whereas the second term of each expression is radiated from all points on the circumference of the disk. Since the point of observation in this case is on the axis, from which any point on the circumference is equidistant, the radiated field from each circumferenical point is equal and all of them add nicely to a single term (the second term of (28a) and (28b)). However, when the observation point is off-axis (i.e. s is finite and nonzero), its distance from different circumferential points is different and, therefore, an infinite number of terms are needed, in general, to represent the total off-axis field or energy density. For $s < 1$ the electric fields have the following representations.

$$E_{xs}(\vec{r},t) = -E_0 \sin\omega_0 t^* \{U(t^*) - U(t^* - T)\}$$

$$+ E_0 \Big[\sum_{m=0}^{\infty} (-1)^m s^{2m} J_{2m} \left(\frac{\pi s}{2\alpha}\right) \sin\omega_0 \{t^* - \frac{\pi(1+s^2)}{4\alpha\omega_0}\}$$

$$- \sum_{m=0}^{\infty} (-1)^m s^{2m+1} J_{2m+1} \left(\frac{\pi s}{2\alpha}\right) \cos\omega_0 \{t^* - \frac{\pi(1+s^2)}{4\alpha\omega_0}\}\Big]$$

$$\cdot [U\{t^* - \frac{\pi(1+s)^2}{4\alpha\omega_0}\} - U\{t^* - \frac{\pi(1+s)^2}{4\alpha\omega_0} - T\}], \tag{29a}$$

where we have used $a^2\omega_0/(cz) = \pi/(2\alpha)$ and

$$E_{xc}(\vec{r},t) = -E_0 \cos\omega_0 t^* \{U(t^*) - U(t^* - T)\}$$

$$+ E_0 \Big[\sum_{m=0}^{\infty} (-1)^m s^{2m} J_{2m} \left(\frac{\pi s}{2\alpha}\right) \cos\omega_0 \{t^* - \frac{\pi(1+s^2)}{4\alpha\omega_0}\}$$

$$- \sum_{m=0}^{\infty} (-1)^m s^{2m+1} J_{2m+1} \left(\frac{\pi s}{2\alpha}\right) \sin\omega_0 \{t^* - \frac{\pi(1+s^2)}{4\alpha\omega_0}\}\Big].$$

$$\cdot \left[U\{t^* - \frac{\pi(1+s)^2}{4\alpha\omega_0} - U\{t^* - \frac{\pi(1+s)^2}{4\alpha\omega_0} - T\} \right]. \qquad (29b)$$

In this case the first terms of (29a) and (29b) also correspond to the radiation directly from the center of the disk. The rest of the infinite series of each expression represents the contributions from every point on the circumference of the disk. For $s = 0$ each of the infinite series reduces to a single term which is equal to the respective second term of (28a) and (28b). Here again (29b) can be obtained by differentiating (29a) with respect to $\omega_0 t^*$. For $s = 1$, using some well known relations involving Bessel functions, the expression (29a) and (29b) can be reduced to (30a) and (30b) respectively. Alternatively, using (18a) into (13) together with (20a) and (20b) the relations (30a) and (30b) can be obtained. Thus for $s = 1$ we have

$$E_{xs}(\rho = a,z,t) = (E_0/2) \left[- \sin \omega_0 t^* \{U(t^*) - U(t^* - T)\} \right.$$

$$\left. + J_0 \left[\frac{\pi}{2\alpha} \right] \sin\omega_0 \left(t^* - \frac{\pi}{2\alpha\omega_0}\right) \{U(t^* - \frac{\pi}{\alpha\omega_0}) - U(t^* - \frac{\pi}{\alpha\omega_0} - T)\} \right], \qquad (30a)$$

and

$$E_{xc}(\rho = a,z,t) = (E_0/2) \left[- \cos\omega_0 t^* \{U(t^*) - U(t^* - T)\} \right.$$

$$\left. + J_0 \left[\frac{\pi}{2\alpha} \right] \cos \omega_0 (t^* - \frac{\pi}{2\alpha\omega_0}) \left\{ U(t^* - \frac{\pi}{\alpha\omega_0}) - U(t^* - \frac{\pi}{\alpha\omega_0} - T) \right\} \right]. \qquad (30b)$$

Noting that $t^* - \frac{\pi}{\alpha\omega_0} = t - (z + 2a^2/z)/c \simeq t - ((2a)^2 + z^2)^{1/2}$, for $2a/z << 1$, one may attempt to point out the origins of each terms of (30a) and (30b) in the following manner. Consider a point P on the cylindrical surface of radius a, the base of this cylindrical surface being the circular disk radiator. Let Q be the intersection of a line through P parallel to the z-axis and the circumference of the circular disk. Then PQ is the z-coordinate of P. Let the point R be on the circumference diametrically opposite to Q, i.e. $QR = 2a$. Then $PR = ((2a)^2 + z^2)^{1/2} \simeq z + 2a^2/z$, for $2a << z$. The first term of (30a) and (30b) shows the portion of the field at P originating from Q.

The second term is contributed by rays from all other circumferential points, the point R having the largest distance from P.

The electric fields for points $s > 1$ can also be expressed in the form of an infinite series similar to (29a) and (29b) using the relations (7) in (13). However, we simply present the dominant term for only $z\sqrt{2/a} >> s >> 1$.

$$E_{xs}(\vec{r},t) \simeq - E_0(1/s)\, J_1\left(\frac{\pi s}{2\alpha}\right) \cos\omega_0 \{t^* - \frac{\pi(1+s^2)}{4\alpha\omega_0}\} \left[U\{t^* - \frac{\pi(1+s)^2}{4\alpha\omega_0}\}\right.$$

$$\left. - U\{t^* - \frac{\pi(1+s)^2}{4\alpha\omega_0} - T\}\right] \tag{31a}$$

and

$$E_{xc}(\vec{r},t) \simeq E_0(1/s)\, J_1\left(\frac{\pi s}{2\alpha}\right) \sin\omega_0 \{t^* - \frac{\pi(1+s^2)}{4\alpha\omega_0}\} \left[U\{t^* - \frac{\pi(1+s)^2}{4\alpha\omega_0}\}\right.$$

$$\left. - U\{t^* - \frac{\pi(1+s)^2}{4\alpha\omega_0} - T\}\right]. \tag{31b}$$

Let us now evaluate the expression for the energy density $P(\vec{r})$ given by (14) for those special cases used in electric field computations. Before proceeding farther let us reexpress (14) in a dimensionless form which is more suitable for numerical computation. Then for both the sinusoidal pulses we have

$$P_s(\vec{r}) = [P_0/(2\alpha^2)] \int_0^\infty \frac{\xi^2 \sin^2(\pi/s)}{(\xi^2 - 1)^2} \, |\hat{I}(\xi,\zeta;\alpha,s)|^2 d\xi. \tag{32a}$$

and

$$P_c(\vec{r}) = [P_0/(2\alpha)^2] \int_0^\infty \frac{\xi^4 \sin^2(\pi/s)}{(\xi^2 - 1)^2} \, |\hat{I}(\xi,\zeta,\alpha,s)|^2 \, d\xi. \tag{32b}$$

where

$$\hat{I}(\xi,\zeta;\alpha,s) = \int_0^1 J_0\left(\frac{\pi s\xi\zeta)}{2\alpha}\right) \exp\left(\frac{i\pi\xi\zeta^2}{4\alpha}\right)\zeta d\zeta. \tag{33}$$

For the special cases where closed from solutions are possible, we shall use (14) together with (20a) and (20b), and the results presented in Appendix B will be employed without further explanations. Thus along the axis of the disk where $s = 0$, we have with the aid of (16b) the expressions for the respective energy densities.

$$P_s(z) = P_0 \left[U(1/8 - \alpha) + \{1 - (1 - \frac{1}{8\alpha})\cos\left(\frac{\pi}{4\alpha}\right) - \frac{\sin\left(\frac{\pi}{4\alpha}\right)}{2\pi}\}U(\alpha - 1/8)\right] \tag{34a}$$

and

$$P_c(z) = P_0 \left[U(1/8 - \alpha) + \{1 - (1 - \frac{1}{8\alpha})\cos\left(\frac{\pi}{4\alpha}\right) + \frac{\sin\left(\frac{\pi}{4\alpha}\right)}{2\pi}\}U(\alpha - 1/8)\right]. \tag{34b}$$

It follows from (34a) and (34b) that for large values of α, for which $\pi/4\alpha << 1$, $P_s(z)$ and $P_c(z)$ behave respectively as

$$P_s(z) \sim P_0\, \pi^2/(32\alpha^2), \tag{35a}$$

and

$$P_c(z) \sim P_0/(4\alpha). \tag{35b}$$

Relations (35a) and (35b) show that in the far end of the Fresnel region the energy along the axis due to a single-cycle sine pulse decreases like $1/z^2$, whereas the single-cycle cosine pulse causes the energy to decay as $1/z$, which is much slower than that for the sine pulse. The corresponding CW energy density (see (24)) behaves like $1/z^2$, which follows from

$$P_{cw}(z) \sim P_0\, \pi^2/(64\alpha^2), \tag{35c}$$

Although both P_s and P_{cw} drop like $1/z^2$ in the far end of the Fresnel region, the energy density associated with the single-cycle sine pulse is double that of CW. This shows that both the single-cycle sine and cosine pulse can really enhance the Fresnel region when compared with the CW signal. Noting the high frequency behaviors of the spectra of the sine and cosine pulses (see (21a) and (21b)), it can be stated that the higher the high frequency content of a pulse, the larger is the extension of the Fresnel region. Although a single-cycle cosine pulse is unrealizable (similar to an ideal rectangular pulse), the result illustrates the fact that the shorter the rise time (which corresponds to amount of high frequency content) of a pulse, the greater is the distance along which the energy density remains highly collimated. This observation suggests that if some realizable pulses can be created having the frequency spectra, the behavior of which lies between $1/\omega^2$ and $1/\omega$, for very large ω, such pulses are potential candidates for the enhancement of the Fresnel region.

Next we present the off-axis energy density in the vicinity of the axis (i.e. for $s << 1$), using (17b) into (14), in the following manner [see the derivations of the integrals (2)-(4) in Appendix B]

$$P_s(\rho,z) = P_0 \sum_{i=1}^{16} I_{s,i}, \qquad s < 1/2 \tag{36a}$$

$$P_c(\rho,z) = P_o \sum_{i=1}^{16} I_{c,i}, \qquad s < 1/2 \tag{36b}$$

where

$$I_{s,1} = -(1/4)\left[\{(2/\pi)\sin\left(\frac{\pi}{4\alpha}\right) - (1/2\alpha)\cos\left(\frac{\pi}{4\alpha}\right)\} J_0\left(\frac{\pi s}{2\alpha}\right)\right. \tag{37a}$$

$$\left. + (s/\alpha)\sin\left(\frac{\pi}{4\alpha}\right) J_1\left(\frac{\pi s}{2\alpha}\right)\right] U(\alpha),$$

$$I_{s,2} = (s/4)\left[\{(4/\pi)\cos\left(\frac{\pi}{4\alpha}\right) + (1/2\alpha)\sin\left(\frac{\pi}{4\alpha}\right)\} J_1\left(\frac{\pi s}{2\alpha}\right)\right. \tag{37b}$$

$$- (s/\alpha)\cos(\pi/4\alpha)\, J_0\left[\frac{\pi s}{2\alpha}\right]]U(\alpha)$$

$$I_{s,3} = (s^2/2)\,[[(3/\pi)\sin\left[\frac{\pi}{4\alpha}\right] - (1/4\alpha)\cos\left[\frac{\pi}{4\alpha}\right]]J_2\left[\frac{\pi s}{2\alpha}\right] \tag{37c}$$

$$+ (s/2\alpha)\, J_1\left[\frac{\pi s}{2\alpha}\right]\sin\left[\frac{\pi}{4\alpha}\right]]U(\alpha),$$

$$I_{s,4} = (1/2)U(\alpha), \tag{37d}$$

$$I_{s,5} = (1/2)\, J_0^2\left[\frac{\pi s}{2\alpha}\right] U(\alpha), \tag{37e}$$

$$I_{s,6} = -(1/8)[[2/\pi)\sin\left[\frac{\pi}{4\alpha}\right] + 2(2 - 1/4\alpha)\cos\left[\frac{\pi s}{2\alpha}\right]]J_0\left[\frac{\pi s}{2\alpha}\right] \tag{37f}$$

$$+ (s/\alpha)\, J_1\left[\frac{\pi s}{2\alpha}\right]\sin\left[\frac{\pi}{4\alpha}\right]]U(\alpha - 1/8 - \frac{s}{4}),$$

$$I_{s,7} = (1/8)[[(2/\pi)\sin\left[\frac{\pi}{4\alpha}\right] - 2(2 + \frac{1}{4\alpha})\cos\left[\frac{\pi}{4\alpha}\right]]\, J_0\left[\frac{\pi s}{2\alpha}\right] \tag{37g}$$

$$+ (s/\alpha)J_1\left[\frac{\pi s}{2\alpha}\right]\sin\left[\frac{\pi s}{2\alpha}\right]]U(\alpha),$$

$$I_{s,8} = (s/8)[[4/\pi)\cos\left[\frac{\pi}{4\alpha}\right] - 2(2 - \frac{1}{4\alpha})\sin\left[\frac{\pi}{4\alpha}\right]]\, J_1\left[\frac{\pi s}{2\alpha}\right] - \tag{37h}$$

$$- (s/\alpha)\, J_0\left[\frac{\pi s}{2\alpha}\right]\cos\left[\frac{\pi}{4\alpha}\right]]U(\alpha - 1/8 - s/4),$$

$$I_{s,9} = -(s/8)\,[[(4/\pi)\cos\left[\frac{\pi}{4\alpha}\right] + 2(2 + \frac{1}{4\alpha})\sin\left[\frac{\pi}{4\alpha}\right]]J_1\left[\frac{\pi s}{2\alpha}\right] \tag{37i}$$

$$- (s/\alpha)J_0\left[\frac{\pi s}{2\alpha}\right]\cos\left[\frac{\pi}{4\alpha}\right]]U(\alpha),$$

$$I_{s,10} = (s^2/2)\, J_1^2 \left[\frac{\pi s}{2\alpha}\right] U(\alpha - s/2), \tag{37j}$$

$$I_{s,11} = -\, s^2\, J_0 \left[\frac{\pi s}{2\alpha}\right] J_2 \left[\frac{\pi s}{2\alpha}\right] U(\alpha - s/2), \tag{37k}$$

$$I_{s,12} = (s^2/8)\,[\{-(6/\pi)\sin\left[\frac{\pi}{4\alpha}\right] + 2(2 - \frac{1}{4\alpha})\cos\left[\frac{\pi}{4\alpha}\right]\} J_2 \left[\frac{\pi s}{2\alpha}\right] \tag{37l}$$

$$+ (s/\alpha)\, J_1 \left[\frac{\pi s}{2\alpha}\right] \sin\left[\frac{\pi}{4\alpha}\right]] U(\alpha - 1/8 - s/4),$$

$$I_{s,13} = (s^2/8)\,[\{(6/\pi)\sin\left[\frac{\pi}{4\alpha}\right] + 2(2 + \frac{1}{4\alpha})\cos\left[\frac{\pi}{2\alpha}\right]\} J_2 \left[\frac{\pi s}{2\alpha}\right] \tag{37m}$$

$$- (s/\alpha)\, J_1 \left[\frac{\pi s}{2\alpha}\right] \sin\left[\frac{\pi}{4\alpha}\right]] U(\alpha),$$

$$I_{s,14} = (1/8)\,[\{2/\pi)\sin\left[\frac{\pi}{4\alpha}\right] + 2(2 - \frac{1}{4\alpha})\cos\left[\frac{\pi}{2\alpha}\right]\} J_0 \left[\frac{\pi s}{2\alpha}\right] \tag{37n}$$

$$+ (s/\alpha)\, J_1 \left[\frac{\pi s}{2\alpha}\right] \sin\left[\frac{\pi}{4\alpha}\right]] U(1/8 - s/4 - 2),$$

$$I_{s,15} = (s/8)[\{-(4/\pi)\cos\left[\frac{\pi}{4\alpha}\right] + 2(2 - \frac{1}{4\alpha})\sin\left[\frac{\pi}{4\alpha}\right]\} J_1 \left[\frac{\pi s}{2\alpha}\right] \tag{37o}$$

$$+ (s/\alpha)\, J_0 \left[\frac{\pi s}{2\alpha}\right] \cos\left[\frac{\pi}{4\alpha}\right]] U(1/8 - \frac{s}{4} - \alpha),$$

$$I_{s,16} = -\,(s^2/8)\,[\{(6/\pi)\sin\left[\frac{\pi}{4\alpha}\right] + 2(2 - \frac{1}{4\alpha})\cos\left[\frac{\pi}{4\alpha}\right]\} J_2 \left[\frac{\pi s}{2\alpha}\right] \tag{37p}$$

$$- (s/\alpha)\, J_1 \left[\frac{\pi s}{2\alpha}\right] \sin\left[\frac{\pi}{4\alpha}\right]]\, U(1/8 - s/4 - \alpha).$$

$$I_{c,1} = (1/4)[\{(2/\pi)\sin\left[\frac{\pi}{4\alpha}\right] + (1/2\alpha)\cos\left[\frac{\pi}{4\alpha}\right]\} J_0 \left[\frac{\pi}{2\alpha}\right] \tag{38a}$$

$$- (s/\alpha) J_1 \left[\frac{\pi s}{2\alpha}\right] \sin \left[\frac{\pi}{4\alpha}\right]]U(\alpha),$$

$$I_{c,2} = - (s/4)[(1/2\alpha) J_1 \left[\frac{\pi s}{2\alpha}\right] \sin \left[\frac{\pi}{4\alpha}\right] \tag{38b}$$

$$+ (s/\alpha) J_0 \left[\frac{\pi s}{2\alpha}\right] \cos \left[\frac{\pi}{4\alpha}\right]]U(\alpha),$$

$$I_{c,3} = - (s^2/4) [\{- (2/\pi) \sin \left[\frac{\pi}{4\alpha}\right] + (1/2\alpha) \cos \left[\frac{\pi}{4\alpha}\right] \} J_2 \left[\frac{\pi s}{2\alpha}\right] \tag{38c}$$

$$+ (s/\alpha) J_1 \left[\frac{\pi s}{2\alpha}\right] \sin \left[\frac{\pi}{4\alpha}\right]]U(\alpha),$$

$$I_{c,4} = (1/2)U(\alpha), \tag{38d}$$

$$I_{c,5} = (1/2) J_0^2 \left[\frac{\pi s}{2\alpha}\right] U(\alpha), \tag{38e}$$

$$I_{c,6} = (1/4) [\{(1/\pi) \sin \left[\frac{\pi}{4\alpha}\right] - 2(2 - 1/4\alpha) \cos \left[\frac{\pi}{4\alpha}\right] \} J_0 \left[\frac{\pi s}{2\alpha}\right] \tag{38f}$$

$$- (s/2\alpha) J_1 \left[\frac{\pi s}{2\alpha}\right] \sin \left[\frac{\pi}{4\alpha}\right]]U(\alpha - \frac{1}{8} - s/4),$$

$$I_{c,7} = - (1/4) [\{1/\pi) \sin \left[\frac{\pi}{4\alpha}\right] + (2 + 1/4\alpha) \cos \left[\frac{\pi}{4\alpha}\right] \} J_0 \left[\frac{\pi s}{2\alpha}\right] \tag{38g}$$

$$- (s/2\alpha) J_1 \left[\frac{\pi s}{2\alpha}\right] \sin \left[\frac{\pi}{4\alpha}\right]] U(\alpha),$$

$$I_{c,8} = - (s/4) [(2 - 1/4\alpha) J_1 \left[\frac{\pi s}{2\alpha}\right] \sin \left[\frac{\pi}{4\alpha}\right] \tag{38h}$$

$$+ (s/2\alpha) J_0 \left[\frac{\pi s}{2\alpha}\right] \cos \left[\frac{\pi}{4\alpha}\right]] U(\alpha - 1/8 - s/4),$$

$$I_{c,9} = -(s/4)\left[(2 + 1/4\alpha) J_1\left(\frac{\pi s}{2\alpha}\right) \sin\left(\frac{\pi}{4\alpha}\right)\right. \tag{38i}$$

$$\left. - (s/2\alpha) J_0\left(\frac{\pi s}{2\alpha}\right) \cos\left(\frac{\pi}{4\alpha}\right)\right] U(\alpha),$$

$$I_{c,10} = (s^2/2) J_1^2\left(\frac{\pi s}{2\alpha}\right) U(\alpha - s/2), \tag{38j}$$

$$I_{c,11} = -s^2 J_0\left(\frac{\pi s}{2\alpha}\right) J_2\left(\frac{\pi s}{2\alpha}\right) U(\alpha - s/2), \tag{38k}$$

$$I_{c,12} = (s^2/4)\left[\left\{(1/\pi) \sin\left(\frac{\pi}{4\alpha}\right) + \left(2 - \frac{1}{4\alpha}\right)\cos\left(\frac{\pi}{4\alpha}\right)\right\} J_2\left(\frac{\pi s}{2\alpha}\right)\right. \tag{38l}$$

$$\left. - (s/2\alpha) J_1\left(\frac{\pi s}{2\alpha}\right) \sin\left(\frac{\pi}{4\alpha}\right)\right] U(\alpha - 1/8 - \frac{s}{4}),$$

$$I_{c,13} = (s^2/4)\left[\left\{-(1/\pi) \sin\left(\frac{\pi}{4\alpha}\right) + \left(2 + \frac{1}{4\alpha}\right) \cos\left(\frac{\pi}{4\alpha}\right)\right\} J_2\left(\frac{\pi s}{2\alpha}\right)\right. \tag{38m}$$

$$\left. + (s/2\alpha) J_1\left(\frac{\pi s}{2\alpha}\right) \sin\left(\frac{\pi}{4\alpha}\right)\right] U(\alpha),$$

$$I_{c,14} = (1/4)\left[\left\{-(1/\pi) \sin\left(\frac{\pi}{4\alpha}\right) + \left(2 - \frac{1}{4\alpha}\right) \cos\left(\frac{\pi}{4\alpha}\right)\right\} J_0\left(\frac{\pi s}{2\alpha}\right)\right. \tag{38n}$$

$$\left. + (s/2\alpha) J_1\left(\frac{\pi s}{2\alpha}\right) \sin\left(\frac{\pi}{4\alpha}\right)\right] U(\frac{1}{8} - \frac{s}{4} - \alpha),$$

$$I_{c,15} = -(s/4)\left[(2 - 1/4\alpha) J_1\left(\frac{\pi s}{2\alpha}\right) \sin\left(\frac{\pi}{4\alpha}\right)\right. \tag{38o}$$

$$\left. + (s/2\alpha) J_0\left(\frac{\pi s}{2\alpha}\right) \cos\left(\frac{\pi}{4\alpha}\right)\right] U(1/8 - \frac{s}{4} - \alpha),$$

$$I_{c,16} = -(s^2/4)\left[\left\{(1/\pi) \sin\left(\frac{\pi}{4\alpha}\right) + (2 - 1/4\alpha) \cos\left(\frac{\pi}{4\alpha}\right)\right\} J_2\left(\frac{\pi s}{2\alpha}\right)\right. \tag{38p}$$

$$- (s/2\alpha)\, J_1 \left[\frac{\pi s}{4\alpha}\right] \sin \left[\frac{\pi}{4\alpha}\right]] \, U(1/8 - s/4 - \alpha). \quad \text{---}$$

Note that for $s = 0$, the relations (36a) and (36b) reduce to (34a) and (34b) respectively. Then for $s = 1$, using (18b) in (14) we have

$$P_s(\rho = a,z) = (P_0/8)\,[1 + J_0^2 \left[\frac{\pi}{2\alpha}\right] - 2J_0 \left[\frac{\pi}{2\alpha}\right] \cos \left[\frac{\pi}{2\alpha}\right]$$

$$+ (1/2\alpha)\,\{J_0 \left[\frac{\pi}{2\alpha}\right] \cos \left[\frac{\pi}{2\alpha}\right] - J_1 \left[\frac{\pi}{2\alpha}\right] \sin \left[\frac{\pi}{2\alpha}\right]\}$$

$$- J_0 \left[\frac{\pi}{2\alpha}\right] \sin \left[\frac{\pi}{2\alpha}\right]/\pi], \; \alpha \geq 1/2. \tag{39a}$$

and

$$P_c(\rho = a,z) = (P_0/8)\,[1 + J_0^2 \left[\frac{\pi}{2\alpha}\right] - 2J_0 \left[\frac{\pi}{2\alpha}\right] \cos \left[\frac{\pi}{2\alpha}\right]$$

$$+ (1/2\alpha)\,\{J_0 \left[\frac{\pi}{2\alpha}\right] \cos \left[\frac{\pi}{2\alpha}\right] - J_1 \left[\frac{\pi}{2\alpha}\right] \sin \left[\frac{\pi}{2\alpha}\right]\}$$

$$+ J_0 \left[\frac{\pi}{2\alpha}\right] \sin \left[\frac{\pi}{2\alpha}\right]/\pi], \; \alpha \geq 1/2. \tag{39b}$$

Finally for $s >> 1$, use of (19b) in (14) yields the following expressions for the energy densities.

$$P_s\,(\rho,z) \simeq P_0\, J_1^2 \left[\frac{\pi s}{2\alpha}\right]/(2s^2) \simeq P_c\,(\rho,z),\; 1 << s < 2\alpha. \tag{40}$$

The conditions, such as $1 << s < 2\alpha$, $U(\alpha - 1/8 - s/4)$ etc., which appear with various expressions indicate the region of validity of that expression in question. These conditions are nothing but the requirements of the convergence of certain integrals, which had to be evaluated in obtaining that expression. In addition, it is also necessary to remember that the validity of the approximation in (2a) used for Fresnel region requires $a^2/(2z) << z$, $a\rho/z << z$ and $\rho^2/(2z) << z$, which

are equivalent to $4\alpha(a/\lambda_0) >> \sqrt{s}$ and $4\alpha(a/\lambda_0) > > s/\sqrt{2}$, for all values of s and α. These later conditions, must therefore, also be imposed simultaneously with those mentioned above.

APPENDIX B

EVALUATION OF CERTAIN INTEGRALS

Special cases of the following integrals involving Bessel, exponential and trigonometric functions appear in the Appendix A.

$$\mathcal{I}_{f,l} = \int_{-\infty}^{\infty} \hat{F}_l(\omega)\, J_n(\beta\omega)\, e^{-i\sigma\omega}\, d\omega, \tag{1}$$

$$\mathcal{I}_{e1,l} = \int_{-\infty}^{\infty} |\hat{F}_l(\omega)|^2\, J_n(\beta\omega)\, J_m(\beta\omega)\, d\omega, \tag{2}$$

$$\mathcal{I}_{e2,l} = \int_{-\infty}^{\infty} |\hat{F}_l(\omega)|^2\, J_n(\beta\omega) \cos(\beta_0\,\omega)\, d\omega, \tag{3}$$

$$\mathcal{I}_{e3,l} = \int_{-\infty}^{\infty} |\hat{F}_l(\omega)|^2\, J_n(\beta\omega) \sin(\beta_0\,\omega)\, d\omega, \tag{4}$$

where β, β_0 and σ are positive; and $l = s$ for the single-cycle sine pulse and $l = c$ for the single-cycle cosine pulse. The frequency spectra of the single-cycle sinusoids are given by

$$\hat{F}_s(\omega) = 2i\,\omega_0\, e^{i\omega T/2} \sin(\omega T/2)/(\omega^2 - \omega_0^2), \tag{5}$$

$$\hat{F}_c(\omega) = -2\omega\, e^{i\omega T/2} \sin(\omega T/2)/(\omega^2 - \omega_0^2), \tag{6}$$

where $\omega_0 T = 2\pi$. Since the functions $\hat{F}_s(\omega)$ and $\hat{F}_c(\omega)$ are bounded (or finite) at $\omega = \pm\,\omega_0$, these points along the real axis of ω are not the singular points (or poles) of any of the above integrals. However, the factor $e^{i\omega T/2} \sin(\omega T/2)$ has different exponential behavior in the upper and lower halves of the complex ω-plane. Therefore, it is necessary to split this factor into exponential form, $(e^{i\omega T} - 1)/(2i)$, and then consider each term of these factors separately for evaluating the resulting integrals. However, this procedure introduces pole singularities at $\omega = \pm\,\omega_0$ on the real ω-axis in each of the separate integrals. In order to avoid this difficulty, we replace the integration path from

$-\infty$ to $+\infty$ in the original integrals (1) to (4) by a path (or contour) C (Fig. 2), which also runs along the real axis except at $\omega = \pm\omega_0$, where upward (i.e. above the real axis) indentations are made, thus avoiding the path running through $\omega = \pm \omega_0$. This is permissible, since the original integrals before spliting the functions $\hat{F}_l(\omega)$ or $|\hat{F}_l(\omega)|^2$ into exponential forms, are analytic in the neighborhood of $\omega = \pm \omega_0$, an appropriate deformation of the path of integration around these points will not change the value of the integrals. Therefore, the original path along the real axis for all the integrals (1) to (4) is replaced by the contour C, described above.

Before evaluating (1) to (4) it will be very helpful to consider the following auxiliary integrals involving Bessel and Hankel functions of integer orders.

$$\mathcal{J}_1 = \int_C \frac{J_n(\beta\omega)}{(\omega^2 - \omega_0^2)} \exp(-i\omega\sigma)\, d\omega,\ \sigma \geq \beta > 0, \tag{7}$$

$$\mathcal{J}_2 = \int_C \omega \frac{J_n(\beta\omega)}{(\omega^2 - \omega_0^2)} \exp(-i\omega\sigma)\, d\omega,\ \sigma \geq \beta > 0, \tag{8}$$

$$\mathcal{J}_3 = \int_C \frac{J_n(\beta\omega)}{(\omega^2 - \omega_0^2)^2} \exp(-i\delta\omega)\, d\omega,\ \delta \geq \beta > 0, \tag{9}$$

$$\mathcal{J}_4 = \int_C \omega^2 \frac{J_n(\beta\omega)}{(\omega^2 - \omega_0^2)^2} \exp(-i\delta\omega)\, d\omega,\ \delta \geq \beta > 0, \tag{10}$$

$$\mathcal{J}_5 = \int_C \frac{J_n(\beta\omega)}{(\omega^2 - \omega_0^2)^2} H_m^{(2)}(\beta\omega)\, d\omega,\ \beta > 0,\ 0 \leq m \leq n, \tag{11}$$

$$\mathcal{J}_6 = \int_C \omega^2 \frac{J_n(\beta\omega)}{(\omega^2 - \omega_0^2)^2} H_m^{(2)}(\beta\omega)\, d\omega,\ \beta > 0,\ 0 \leq m \leq n + 2, \tag{12}$$

$$\mathcal{J}_7 = \int_C \frac{J_n(\beta\omega)}{(\omega^2 - \omega_0^2)^2} J_m(\beta\omega) \exp(-i\sigma\omega),\ \sigma \geq 2\beta > 0, \tag{13}$$

$$\mathcal{J}_8 = \int_C \omega^2 \frac{J_n(\beta\omega)}{(\omega^2 - \omega_0^2)^2} J_m(\beta\omega) \exp(-i\sigma\omega),\ \sigma > 2\beta > 0. \tag{14}$$

The contour C of the above integrals (7)-(14) can be joined by an infinite semi-circle in the lower half of the complex ω-plane. The integrands on the infinite semi-circle vanish either exponentially or at least as $\omega^{-3/2}$. The branch cut of $H_m^{(2)}(\beta\omega)$ in (11) and (12) is chosen along a ray (starting at the origin $\omega = 0$) in the 2nd guadrant of the ω-plane, making a very small angle with the negative real axis, so that the branch cut does not touch the indented contour C. In order to avoid the branch cut, the contour C in (11) and (12) is indented also below the origin, although they are not shown in Fig. 2. It may also be noted that imposition of various convergence conditions, such as $o \leq m \leq n$, $o \leq m \leq n + 2$, $\sigma \geq \beta > 0$, $\delta \geq \beta > 0$ and $\sigma \geq 2\beta > 0$, the behaviors of the Bessel and Hankel functions in the complex ω-plane played a role. With these preliminary observations, the preceeding integrals can be evaluated easily by the application of the calculus of residue. In particular, if $N(\omega)$ represents any of the numerators of the integrands of $\mathcal{I}_3$ to $\mathcal{I}_8$, then the value of those integrals can be expressed as

$$(-2\pi i)\left[\frac{d}{d\omega}\left\{N(\omega)/(\omega-\omega_0)^2\right\}_{\omega=-\omega_0} + \frac{d}{d\omega}\left\{N(\omega)/(\omega+\omega_0)^2\right\}_{\omega=\omega_0}\right]. \tag{15}$$

Following the procedure outlined above, the integrals (7) to (14) can be evaluated as presented below.

$$\mathcal{I}_1 = \begin{cases}(-2\pi/\omega_0)\, J_n(\beta\omega_0)\sin(\omega_0\sigma)\, U(\sigma-\beta), \\ \text{for } n = 0, \text{ or even integer,}\end{cases} \tag{16a}$$

$$= \begin{cases}-(2\pi i/\omega_0)\, J_n(\beta\omega_0)\cos(\omega_0\sigma)\, U(\sigma-\beta), \\ \text{for } n = \text{odd integer,}\end{cases} \tag{16b}$$

$$\text{where } U(x) = \begin{cases}1, \text{ for } x \geq 0 \\ 0, \text{ for } x < 0\end{cases} \tag{17}$$

$$\mathcal{I}_2 = \begin{cases}(-2\pi i)\, J_n(\beta\omega_0)\cos(\omega_0\sigma)\, U(\sigma-\beta) \\ \text{for} n = 0, \text{ or even integer,}\end{cases} \tag{18a}$$

$$= \begin{cases} (-2\pi)\, J_n\,(\beta\omega_0) \sin\,(\omega_0\,\sigma)\, U(\sigma - \beta) \\ \text{for } n = \text{odd integer.} \end{cases} \tag{18b}$$

$$\mathcal{J}_3 = \begin{cases} (\pi/\omega_0^3)\,[(n+1)\, J_n\,(\beta\,\omega_0) \sin\,(\delta\,\omega_0) - \beta\,\omega_0\, J_{n-1}\,(\beta\omega_0) \sin\,(\delta\omega_0) \\ -\delta\omega_0\, J_n\,(\beta\omega_0) \cos\,(\delta\omega_0)]\, U\,(\delta - \beta), \\ \text{for } n = 0, \text{ or even integer,} \end{cases} \tag{19a}$$

$$= \begin{cases} (i\pi/\omega_0^3)\,[(n+1)\, J_n\,(\beta\omega_0) \cos\,(\delta\,\omega_0) - \beta\omega_0\, J_{n-1}\,(\beta\omega_0) \cos\,(\delta\omega_0) \\ +\,\delta\,\omega_0\, J_n\,(\beta\omega_0) \sin\,(\delta\,\omega_0)]\, U(\delta - \beta) \\ \text{for } n = \text{odd integer.} \end{cases} \tag{19b}$$

$$\mathcal{J}_4 = \begin{cases} (\pi/\omega_0)\,[(n-1)\, J_n\,(\beta\omega_0) \sin\,(\delta\omega_0) - \beta\omega_0\, J_{n-1}\,(\beta\omega_0) \sin\,(\delta\omega_0) \\ -\,\delta\omega_0\, J_n\,(\beta\omega_0) \cos\,(\delta\omega_0)]\, U\,(\delta - \beta) \\ \text{for } n = 0, \text{ or even integer,} \end{cases} \tag{20a}$$

$$= \begin{cases} (i\pi/\omega_0)\,[(n-1)\, J_n\,(\beta\omega_0) \cos\,(\delta\omega_0) - \beta\omega_0\, J_{n-1}(\beta\omega_0) \cos\,(\delta\,\omega_0) \\ +\,\delta\omega_0\, J_n\,(\beta\omega_0) \sin\,(\delta\omega_0)]\, U\,(\delta - \beta), \\ \text{for } n = \text{odd integer.} \end{cases} \tag{20b}$$

$$\mathcal{J}_5 = \begin{cases} (i\pi/\omega_0^3)\,[\{(n+m+1)\, J_n\,(\beta\omega_0) - \beta\omega_0\, J_{n-1}\,(\beta\omega_0)\}\, J_m\,(\beta\omega_0) \\ -\,\beta\omega_0\, J_n\,(\beta\omega_0)\, J_{m-1}\,(\beta\omega_0)] \\ \text{for } n + m = 0, \text{ or even integer,} \end{cases} \tag{21a}$$

$$= \begin{cases} (\pi/\omega_0^3)\,[\{(n+m+1)\, J_n\,(\beta\omega_0) - \beta\omega_0\, J_{n-1}(\beta\omega_0)\}\, N_m\,(\beta\omega_0) \\ -\,\beta\omega_0\, J_n\,(\beta\omega_0)\, N_{m-1}\,(\beta\omega_0)] \\ \text{for } n + m = \text{odd integer,} \end{cases} \tag{21b}$$

where $N_m(\beta\omega_0)$ and $N_{m-1}(\beta\omega_0)$ are Neumann's functions.

Taking now the real and imaginary parts of (11) and (21) we have

$$\mathcal{J}_{5a} = \int_C \frac{J_n(\beta\omega)\, J_m\,(\beta\omega) d\omega}{(\omega^2 - \omega_0)^2}$$

$$= \begin{cases} 0, \text{for } n + m = 0, \text{ or even integer,} \\ 0 \le m \le n, \end{cases} \tag{22a}$$

$$= \begin{cases} (\pi/\omega_0^3)\,[\{(n+m+1)\,J_n(\beta\omega_0) - \beta\omega_0\,J_{n+1}(\beta\omega_0)\}N_m(\beta\omega_0) \\ -\beta\omega_0\,J_n(\beta\omega_0)\,N_{m-1}(\beta\omega_0)] \\ \text{for } n+m = \text{odd integer}, \\ 0 \le m \le n, \end{cases} \tag{22b}$$

and

$$\mathcal{I}_{5b} = \int_C \frac{J_n(\beta\omega)\,N_m(\beta\omega)\,d\omega}{(\omega^2 - \omega_0^2)^2}$$

$$= \begin{cases} (\pi/\omega_0^3)[\{-(n+m+1)\,J_n(\beta\omega_0) + \beta\omega_0\,J_{n-1}(\beta\omega_0)\}J_m(\beta\omega_0) \\ +\beta\omega_0 J_n(\beta\omega_0)\,J_{m-1}(\beta\omega_0)] \\ \text{for } n+m = 0, \text{ or even } \textit{integer}, \\ 0 \le m \le n, \end{cases} \tag{23a}$$

$$= 0, \text{for } n+m = \text{odd integer. } 0 \le m \le n. \tag{23b}$$

$$\mathcal{I}_6 = \begin{cases} (-i\pi/\omega_0)[\{-(n+m-1)\,J_n(\beta\omega_0) + \beta\omega_0\,J_{n-1}(\beta\omega_0)\}\,J_m(\beta\omega_0) \\ +\beta\omega_0\,J_n(\beta\omega_0)\,J_{m-1}(\beta\omega_0)], \\ \text{for } n+m = 0, \text{ or even integer} \\ 0 \le m \le n+2 \end{cases} \tag{24a}$$

$$= \begin{cases} (-\pi/\omega_0)\,[\{-(n+m-1)\,J_n(\beta\omega_0) + \beta\omega_0\,J_{n-1}(\beta\omega_0)\}\,N_m(\beta\omega_0) \\ +\beta\omega_0\,J_n(\beta\omega_0)\,N_{m-1}(\beta\omega_0)] \\ \text{for } n+m = \text{odd integer}, \ 0 \le m \le n+2. \end{cases} \tag{24b}$$

Equating real and imaginary parts of (12) and (24) we have

$$\mathcal{I}_{6a} = \int_C \frac{\omega^2 J_n(\beta\omega)\,J_m(\beta\bar{\omega})}{(\omega^2 - \omega_0^2)^2}\,d\omega, \ 0 \le m \le n+2$$

$$= \begin{cases} 0, \text{ for } n+m = 0, \text{ or even integer} \end{cases} \tag{25a}$$

$$= \begin{cases} (-\pi/\omega_0)[\{-(n+m-1)\,J_n(\beta\omega_0) + \beta\omega_0\,J_{n-1}(\beta\omega_0)\}N_m(\beta\omega_0) \\ +\beta\omega_0\,J_n(\beta\omega_0)\,N_{m-1}(\beta\omega_0)] \\ \text{for } n+m = \text{odd integer}. \end{cases} \tag{25b}$$

$$\mathcal{I}_{6b} = \int_C \frac{\omega^2 J_n(\beta\omega) N_m(\beta\omega) d\omega}{(\omega^2 - \omega_0^2)^2},\ 0 \le m \le n+2$$

$$= \begin{cases} (\pi/\omega_0)[-(n+m-1)J_n(\beta\omega_0) + \beta\omega_0 J_{n-1}(\beta\omega_0)] J_m(\beta\omega_0) \\ + \beta\omega_0 J_n(\beta\omega_0) J_{m-1}(\beta\omega_0)] \\ \text{for } n+m = 0, \text{ or even integer.} \end{cases} \tag{26a}$$

$$= \begin{cases} 0, \text{ for } n+m = \text{odd } \textit{integer} \end{cases} \tag{26b}$$

$$\mathcal{I}_7 = \begin{cases} (\pi/\omega_0^3)[(n+m+1)J_n(\beta\omega_0) J_m(\beta\omega_0) \sin(\sigma\omega_0) \\ - \beta\omega_0 \{J_{n-1}(\beta\omega_0) J_m(\beta\omega_0) + J_n(\beta\omega_0) J_{m-1}(\beta\omega_0)\} \sin(\sigma\omega_0) \\ - \sigma\omega_0 J_n(\beta\omega_0) J_m(\beta\omega_0) \cos(\sigma\omega_0)] U(\sigma - 2\beta), \\ \text{for } n+m = 0, \text{ or even integer,} \end{cases} \tag{27a}$$

$$= \begin{cases} (i\pi/\omega_0^3)[(n+m+1) J_n(\beta\omega_0) J_m(\beta\omega_0) \cos(\sigma\omega_0) \\ - \beta\omega_0 \{J_{n-1}(\beta\omega_0) J_m(\beta\omega_0) + J_n(\beta\omega_0) J_{m-1}(\beta\omega_0)\} \cos(\sigma\omega_0) \\ + \sigma\omega_0 J_n(\beta\omega_0) J_m(\beta\omega_0) \sin(\sigma\omega_0)] U(\sigma - 2\beta) \\ \text{for } n+m = \text{odd integer.} \end{cases} \tag{27b}$$

$$\mathcal{I}_8 = \begin{cases} (-i\pi/\omega_0)[\{-(n+m-1) J_n(\beta\omega_0) + \beta\omega_0 J_{n-1}(\beta\omega_0)\} J_m(\beta\omega_0) \\ + \beta\omega_0 J_n(\beta\omega_0) J_{m-1}(\beta\omega_0)] U(\sigma - 2\beta) \\ \text{for } n+m = 0, \text{ or even integer,} \end{cases} \tag{28a}$$

$$= \begin{cases} (-\pi/\omega_0)[\{-(n+m-1) J_n(\beta\omega_0) + \beta\omega_0 J_{n-1}(\beta\omega_0)\} N_m(\beta\omega_0) \\ + \beta\omega_0 J_n(\beta\omega_0) N_{m-1}(\beta\omega_0)] U(\sigma - 2\beta) \\ \text{for } n+m = \text{odd integer.} \end{cases} \tag{28b}$$

In addition, the following relations can be easily established.

$$\mathcal{I}_9 = \int_C \frac{J_n(\beta\omega) e^{i\omega\sigma} d\omega}{(\omega^2 - \omega_0^2)} = 0,\ \sigma > \beta > 0, \tag{29}$$

$$\mathcal{I}_{10} = \int_C \frac{\omega J_n(\beta\omega) e^{i\omega\sigma} d\omega}{(\omega^2 - \omega_0^2)} = 0,\ \sigma > \beta > 0 \tag{30}$$

$$\mathcal{I}_{11} = \int_C \frac{J_n(\beta\omega)\, e^{i\delta\omega} d\omega}{(\omega^2 - \omega_0^2)^2} = 0, \delta > \beta > 0 \tag{31}$$

$$\mathcal{I}_{12} = \int_C \frac{\omega^2\, J_n(\beta\omega)\, e^{i\delta\omega} d\omega}{(\omega^2 - \omega_0^2)^2} = 0, \delta > \beta > 0, \tag{32}$$

$$\mathcal{I}_{13} = \int_C \frac{J_n(\beta\omega)\, H_m^{(1)}(\beta\omega) d\omega}{(\omega^2 - \omega_0^2)^2} = 0,\ \beta > 0,\ 0 \le m \le n \tag{33}$$

$$\mathcal{I}_{14} = \int_C \frac{\omega^2\, J_n(\beta\omega)\, H_m^{(1)}(\beta\omega) d\omega}{(\omega^2 - \omega_0^2)^2} = 0,\ \beta > 0,\ 0 \le m \le n + 2. \tag{34}$$

For (33) and (34) the contour C is also indented above the origin and the branch cut of $H_m^{(1)}(\beta\omega)$ is chosen along a ray from $\omega = 0$ to $-\infty$ slightly below C in the 3rd quadrant.

$$\mathcal{I}_{15} = \int_C \frac{J_n(\beta\omega)\, J_m(\beta\omega) e^{i\sigma\omega} d\omega}{(\omega^2 - \omega_0^2)^2} = 0,\ \sigma > 2\beta > 0 \tag{35a}$$

$$\mathcal{I}_{16} = \int_C \frac{\omega^2\, J_n(\beta\omega)\, J_m(\beta\omega) e^{i\sigma\omega}\, d\omega}{(\omega^2 - \omega_0^2)^2} = 0,\ \sigma > 2\beta > 0. \tag{35b}$$

For all of the integrals (29) to (35), the contour C can be closed by an infinite semi-circle in the upper half of the complex ω-plane. Since all of the integrands vanish on this infinite circle and the integrands are analytic inside the closed contour, the integrals vanish. Furthermore, we have

$$\mathcal{I}_{17} = \int_C \frac{d\omega}{(\omega^2 - \omega_0^2)^2} = 0, \tag{36}$$

$$\mathcal{I}_{18} = \int_C \frac{e^{i\omega T} d\omega}{(\omega^2 - \omega_0^2)^2} = 0, T > 0 \tag{37}$$

$$\mathcal{I}_{19} = \int_C \frac{e^{-i\omega T}}{(\omega^2 - \omega_0^2)^2} = -\pi T/\omega_0^2, T > 0 \tag{38}$$

$$\mathcal{I}_{20} = \int_C \frac{e^{-i\omega \hat{t}}}{(\omega^2 - \omega_0^2)} d\omega = -\left[\frac{2\pi}{\omega_0}\right] \sin \omega_0 \hat{t} \cdot U(\hat{t}) \tag{39}$$

$$\mathcal{I}_{21} = \int_C \frac{\omega\, e^{-i\omega \hat{t}}}{(\omega^2 - \omega_0^2)} = -2\pi i \cos \omega_0 \hat{t}\, U(\hat{t}) \tag{40}$$

In view of (7) and (35), we have the following relations.

$$\mathcal{I}_{22} = \int_C \frac{J_n(\beta\omega)\, J_m(\beta\omega) \cos(\sigma\omega)\, d\omega}{(\omega^2 - \omega_0^2)^2} = \mathcal{I}_7/2,\ \sigma > 2\beta > 0, \tag{41}$$

$$\mathcal{I}_{23} = \int_C \frac{J_n(\beta\omega)\, J_m(\beta\omega) \sin(\sigma\omega)\, d\omega}{(\omega^2 - \omega_0^2)^2} = -\mathcal{I}_7/(2i),\ \sigma > 2\beta > 0. \tag{42}$$

Similarly, from (9) and (31), we have

$$\mathcal{I}_{24} = \int_C \frac{J_n(\beta\omega) \cos(\delta\omega)\, d\omega}{(\omega^2 - \omega_0^2)^2} = \mathcal{I}_3/2,\ \delta > \beta > 0 \tag{43}$$

$$\mathcal{I}_{25} = \int_C \frac{J_n(\beta\omega) \sin(\delta\omega)\, d\omega}{(\omega^2 - \omega_0^2)^2} = -\mathcal{I}_3/(2i),\ \delta > \beta > 0, \tag{44}$$

From (10 and (32), we have

$$\mathcal{I}_{26} = \int_C \frac{\omega^2 J_n(\beta\omega) \cos(\delta\omega)\, d\omega}{(\omega^2 - \omega_0^2)^2} = \mathcal{I}_4/2,\ \delta > \beta > 0, \tag{45}$$

$$\mathcal{I}_{27} = \int_C \frac{\omega^2 J_n(\beta\omega) \sin(\delta\omega)\, d\omega}{(\omega^2 - \omega_0^2)^2} = -\mathcal{I}_4/(2i),\ \delta > \beta > 0, \tag{46}$$

Similarly, from (14) and (35), the following relations can be obtained.

$$\mathcal{I}_{28} = \int_C \frac{\omega^2 J_n(\beta\omega)\, J_m(\beta\omega) \cos(\sigma\omega)\, d\omega}{(\omega^2 - \omega_0^2)^2} = \mathcal{I}_8/2,\ \sigma > 2\beta > 0, \tag{47}$$

$$\mathcal{I}_{29} = \int_C \frac{\omega^2 J_n(\beta\omega)\, J_m(\beta\omega) \sin(\sigma\omega a)\, d\omega}{(\omega^2 - \omega_0^2)^2} = -\mathcal{I}_8/(2i),\ \sigma > 2\sigma > 0. \tag{48}$$

Using now the preceeding results we present the integrals (1) to (4) for $l = s$ and c in the following manner.

$$\mathcal{I}_{f,s} = \int_{-\infty}^{\infty} \hat{F}_s(\omega)\, J_n(\beta\omega)\, e^{-i\sigma\omega}\, d\omega$$

$$= \begin{cases} 2\pi J_n(\beta\omega_0) \sin(\omega_0\sigma)\, [U(\sigma - \beta) - U(\sigma - \beta - T)] \\ \text{for } n = 0 \text{ or even integer,} \end{cases} \tag{49a}$$

$$= \begin{cases} 2\pi i\, J_n(\beta\omega_0)\cos(\omega_0\sigma)\,[U(\sigma-\beta)-U(\sigma-\beta-T)] \\ \text{for } n = \text{odd integer.} \end{cases} \tag{49b}$$

$$\mathcal{I}_{f,c} = \int_{-\infty}^{\infty} \hat{F}_c(\omega)\, J_n(\beta\omega)\, e^{-i\sigma\omega}\, d\omega$$

$$= \begin{cases} 2\pi\, J_n(\beta\omega_0)\cos(\sigma\omega_0)\,[U(\sigma-\beta)-U(\sigma-\beta-T)] \\ \text{for } n = 0, \text{ or even integer,} \end{cases} \tag{50a}$$

$$= \begin{cases} -2\pi i\, J_n(\beta\omega_0)\sin(\sigma\omega_0)\,[U(\sigma-\beta)-U(\sigma-\beta-T)] \\ \text{for } n = \text{odd integer,} \end{cases} \tag{50b}$$

$$\mathcal{I}_{e1,s} = \int_{-\infty}^{\infty} |\hat{F}_s(\omega)|^2\, J_n(\beta\omega)\, J_m(\beta\omega)\, d\omega$$

$$= \begin{cases} (2\pi^2/\omega_0)\, J_n(\beta\omega_0)\, J_m(\beta\omega_0)\, U(\pi/\omega_0-\beta) \\ \text{for } n+m = 0, \text{ or even integer,} \end{cases} \tag{51a}$$

$$= \begin{cases} -(2\pi/\omega_0)\,[\{-(n+m+1)\, J_n(\beta\omega_0)+\beta\omega_0\, J_{n-1}(\beta\omega_0)\}N_m(\beta\omega_0) \\ +\beta\omega_0\, J_n(\beta\omega_0)\, N_{m-1}(\beta\omega_0)]U(\beta) \\ +(i\pi/\omega_0)\,[-(n+m+1)\, J_n(\beta\omega_0)\, J_m(\beta\omega_0)+\beta\omega_0\, J_{n-1}(\beta\omega_0)\, J_m(\beta\omega_0) \\ +\beta\omega_0\, J_n(\beta\omega_0)\, J_{m-1}(\beta\omega_0)]\, U(\pi/\omega_0-\beta) \\ \text{for } n+m = \text{odd integer.} \end{cases} \tag{51b}$$

$$I_{e1,c} = \int_{-\infty}^{\infty} |\hat{F}_c(\omega)|^2\, J_n(\beta\omega)\, J_m(\beta\omega)\, d\omega$$

$$= \begin{cases} (2\pi^2/\omega_0)\, J_n(\beta\omega_0)\, J_m(\beta\omega_0)\, U(\pi/\omega_0-\beta) \\ \text{for } n+m = 0, \text{ for even integer} \end{cases} \tag{52a}$$

$$= \begin{cases} 2\pi/\omega_0)\,[\{(n+m+1)\, J_n(\beta\omega_0)-\beta\omega_0\, J_{n-1}(\beta\omega_0)\}\, N_m(\beta\omega_0) \\ -\beta\omega_0\, J_n(\beta\omega_0)\, N_{m-1}(\beta\omega_0)]\, U(\beta) \\ -(i\pi/\omega_0)\,[\{(n+m-1)\, J_n(\beta\omega_0)-\beta\omega_0\, J_{n-1}(\beta\omega_0)\}\, J_m(\beta\omega_0) \\ -\beta\omega_0\, J_n(\beta\omega_0)\, J_{m-1}(\beta\omega_0)\}]\, U(\pi/\omega_0-\beta) \\ \text{for } n+m = \text{odd integer.} \end{cases} \tag{52b}$$

$$\mathcal{I}_{e2,s} = \int_{-\infty}^{\infty} |\hat{F}_s(\omega)|^2\, J_n(\beta\omega)\cos(\beta_0\omega)\, d\omega$$

$$= (\pi/2\omega_0)\,[(n+1)\, J_n(\beta\omega_0)\sin(\beta_0\omega_0)-\beta\omega_0\, J_{n-1}(\beta\omega_0)\sin(\beta_0\omega_0)$$

$$+ (2\pi - \beta_0 \omega_0) J_n (\beta\omega_0) \cos (\beta_0 \omega_0)] U (2\pi/\omega_0 - \beta_0 - \beta)$$

$$+ (\pi/\omega_0) [(n + 1) J_n (\beta \omega_0) \sin (\beta_0 \omega_0) - \beta \omega_0 J_{n-1} (\beta \omega_0) \sin (\beta_0 \omega_0)$$

$$- \beta_0 \omega_0 J_n (\beta \omega_0) \cos (\beta_0 \omega_0)] U(\beta_0 - \beta)$$

$$+ (\pi/2\omega_0) [- (n + 1) J_n (\beta \omega_0) \sin (\beta_0 \omega_0) + \beta \omega_0 J_{n-1} (\beta \omega_0) \sin (\beta_0 \omega_0)$$

$$+ (\beta_0 \omega_0 - 2\pi) J_n (\beta \omega_0) \cos (\beta_0 \omega_0)] U (\beta_0 - 2\pi/\omega_0 - \beta)$$

$$+ (\pi/2\omega_0) [- (n + 1) J_n (\beta\omega_0) \sin (\beta_0 \omega_0) + \beta \omega_0 J_{n-1} (\beta \omega_0) \sin (\beta_0 \omega_0)$$

$$+ (2\pi + \beta_0\omega_0) J_n (\beta \omega_0) \cos (\beta_0 \omega_0)] U (2\pi/\omega_0 + \beta_0 - \beta)$$

when $n = 0$, or even integer. (53a)

$$= (i\pi/2\omega_0) [- (n + 1) J_n (\beta \omega_0) \cos (\beta_0 \omega_0) + \beta \omega_0 J_{n-1} (\beta \omega_0) \cos (\beta_0 \omega_0)$$

$$+ (2\pi - \beta_0\omega_0) J_n (\beta \omega_0) \sin (\beta_0 \omega_0)]U (2\pi/\omega_0 - \beta_0 - \beta)$$

$$+ (i\pi/\omega_0) [(n + 1) J_n (\beta \omega_0) \cos (\beta_0 \omega_0) - \beta \omega_0 J_{n-1} (\beta \omega_0) \cos (\beta_0 \omega_0)$$

$$+ \beta_0 \omega_0 J_n (\beta \omega_0) \sin (\beta_0 \omega_0)] U (\beta_0 - \beta)$$

$$+ (i\pi/2\omega_0)[- (n + 1) J_n (\beta\omega_0) \cos (\beta_0 \omega_0) + \beta \omega_0 J_{n-1} (\beta \omega_0) \cos (\beta_0 \omega_0)$$

$$+ (\beta_0 \omega_0 - 2\pi) J_n (\beta \omega_0) \sin (\beta_0 \omega_0)] U (\beta_0 - 2\pi/\omega_0 - \beta)$$

$$+ (i\pi/2\omega_0) [- (n + 1) J_n (\beta \omega_0) \cos (\beta_0 \omega_0) + \beta_0 \omega_0 J_{n-1} (\beta\omega_0) \cos (\beta_0 \omega_0)$$

$$- (2\pi + \beta_0 \omega_0) J_n (\beta \omega_0) \sin (\beta_0 \omega_0)] U (2\pi/\omega_0 - \beta_0 - \beta), \quad (53b)$$

when n = odd integer

$$\mathcal{I}_{e2,c} = \int_{-\infty}^{\infty} |\hat{F}_c(\omega)|^2 J_n (\beta\omega) \cos (\beta_0 \omega_0) d \omega$$

$$= (\pi/2\omega_0)\,[(n-1)\,J_n(\beta\,\omega_0)\sin(\beta_0\,\omega_0) - \beta\omega_0\,J_{n-1}(\beta\omega_0)\sin(\beta_0\,\omega_0)$$

$$+ (2\pi - \beta_0\,\omega_0)\,J_n(\beta\,\omega_0)\cos(\beta_0\,\omega_0)]\,U(2\pi/\omega_0 - \beta_0 - \beta)$$

$$+ (\pi/\omega_0)\,[(n-1)\,J_n(\beta\omega_0)\sin\beta_0\omega_0 - \beta\,\omega_0\,J_{n-1}(\beta\,\omega_0)\sin(\beta_0\,\omega_0)$$

$$- \beta_0\,\omega_0\,J_n(\beta\,\omega_0)\cos(\beta_0\,\omega_0)]\,U(\beta_0 - \beta)$$

$$+ (\pi/2\omega_0)\,[-(n-1)J_n(\beta\,\omega_0)\sin(\beta_0\,\omega_0) + \beta\,\omega_0\,J_{n-1}(\beta\,\omega_0)\sin(\beta_0\,\omega_0)$$

$$+ (\beta_0\,\omega_0 - 2\pi)\,J_n(\beta\,\omega_0)\cos(\beta_0\,\omega_0)]\,U(\beta_0 - 2\pi/\omega_0 - \beta)$$

$$+ (\pi/2\omega_0)\,[-(n-1)\,J_n(\beta\omega_0)\sin(\beta_0\,\omega_0) + \beta\,\omega_0\,J_{n-1}(\beta\,\omega_0)\sin(\beta_0\,\omega_0)$$

$$+ (2\pi + \beta_0\,\omega_0)\,J_n(\beta_0\,\omega_0)\cos(\beta_0\,\omega_0)]\,U(2\pi/\omega_0 + \beta_0 - \beta) \qquad (54a)$$

when $n = 0$ or even integer,

$$= (i\pi/2\omega_0)\,[-(n-1)\,J_n(\beta\,\omega_0)\cos(\beta_0\,\omega_0) + \beta\,\omega_0\,J_{n-1}(\beta\,\omega_0)\cos(\beta_0\,\omega_0)$$

$$+ (2\pi - \beta_0\,\omega_0)\,J_n(\beta\,\omega_0)\sin(\beta_0\,\omega_0)]\,U(2\pi/\omega_0 - \beta_0 - \beta)$$

$$+ (i\pi/\omega_0)\,[(n-1)J_n(\beta\,\omega_0)\cos(\beta_0\,\omega_0) - \beta\,\omega_0\,J_{n-1}(\beta\omega_0)\cos(\beta_0\,\omega_0)$$

$$+ \beta_0\,\omega_0\,J_n(\beta\,\omega_0)\sin(\beta_0\,\omega_0)]\,U(\beta_0 - \beta)$$

$$+ (i\pi/2\omega_0)\,[-(n-1)\,J_n(\beta\omega_0)\cos(\beta_0\,\omega_0) + \beta\omega_0\,J_{n-1}(\beta\,\omega_0)\cos(\beta_0\,\omega_0)$$

$$+ (\beta_0\,\omega_0 - 2\pi)\,J_n(\beta\omega_0)\sin(\beta_0\,\omega_0)]\,U(\beta_0 - 2\pi/\omega_0 - \beta)$$

$$+ (i\pi/2\omega_0)[-(n-1)\,J_n(\beta\omega_0)\cos(\beta_0\,\omega_0) + \beta\omega_0\,J_{n-1}(\beta\omega_0)\cos(\beta_0\,\omega_0)$$

$$- (2\pi + \beta_0\,\omega_0)\,J_n(\beta\,\omega_0)\sin(\beta_0\,\omega_0)]\,U(2\pi/\omega_0 + \beta_0 - \beta), \qquad (54b)$$

when n = odd integer.

$$\mathcal{I}_{e3,s} = \int_{-\infty}^{\infty} |\hat{F}_s(\omega)|^2 J_n(\beta\omega) \sin(\beta_0\omega)\, d\omega$$

$$= (i\pi/2\omega_0)[-(n+1)J_n(\beta\omega_0)\sin(\beta_0\omega_0) + \beta\omega_0 J_{n-1}(\beta\omega_0)\sin(\beta_0\omega_0)$$

$$- (2\pi - \beta_0\omega_0) J_n(\beta\omega_0)\cos(\beta_0\omega_0)]\, U(2\pi/\omega_0 - \beta_0 - \beta)$$

$$+ (i\pi/\omega_0)[(n+1) J_n(\beta\omega_0)\sin(\beta_0\omega_0) - \beta\omega_0 J_{n-1}(\beta\omega_0)\sin(\beta_0\omega_0)$$

$$- \beta_0\omega_0 J_n(\beta\omega_0)\cos(\beta_0\omega_0)]\, U(\beta_0 - \beta)$$

$$+ (i\pi/2\omega_0)[-(n+1)J_n(\beta\omega_0)\sin(\beta_0\omega_0) + \beta\omega_0 J_{n-1}(\beta\omega_0)\sin(\beta_0\omega_0)$$

$$+ (\beta_0\omega_0 - 2\pi) J_n(\beta\omega_0)\cos(\beta_0\omega_0)]\, U(\beta_0 - 2\pi/\omega_0 - \beta)$$

$$+ (i\pi/2\omega_0)[-(n+1) J_n(\beta\omega_0)\sin(\beta_0\omega_0) + \beta\omega_0 J_{n-1}(\beta\omega_0)\sin(\beta_0\omega_0)$$

$$+ (2\pi + \beta_0\omega_0) J_n(\beta\omega_0)\cos(\beta_0\omega_0)]\, U(2\pi/\omega_0 + \beta_0 - \beta)$$

when $n = 0$, or even integer, (55a)

$$= (\pi/2\omega_0)[-(n+1) J_n(\beta\omega_0)\cos(\beta_0\omega_0) + \beta\omega_0 J_{n-1}(\beta\omega_0)\cos(\beta_0\omega_0)$$

$$+ (2\pi - \beta_0\omega_0) J_n(\beta\omega_0)\sin(\beta_0\omega_0)]\, U(2\pi/\omega_0 - \beta_0 - \beta)$$

$$+ (\pi/\omega_0)[-(n+1) J_n(\beta\omega_0)\cos(\beta_0\omega_0) + \beta\omega_0 J_{n-1}(\beta\omega_0)\cos(\beta_0\omega_0)$$

$$- \beta_0\omega_0 J_n(\beta\omega_0)\sin(\beta_0\omega_0)]\, U(\beta_0 - \beta)$$

$$+ (\pi/2\omega_0)[(n+1) J_n(\beta\omega_0)\cos(\beta_0\omega_0) - \beta\omega_0 J_{n-1}(\beta\omega_0)\cos(\beta_0\omega_0)$$

$$- (\beta_0\omega_0 - 2\pi) J_n(\beta\omega_0)\sin(\beta_0\omega_0)]\, U(\beta_0 - 2\pi/\omega_0 - \beta)$$

$$+ (\pi/2\omega_0)[(n+1) J_n(\beta\omega_0)\cos(\beta_0\omega_0) - \beta\omega_0 J_{n-1}(\beta\omega_0)\cos(\beta_0\omega_0)$$

$$+ (2\pi + \beta_0\omega_0) J_n(\beta\omega_0)\sin(\beta_0\omega_0)]\, U(2\pi/\omega_0 + \beta_0 - \beta)$$ (55b)

when n = odd integer.

$$\mathcal{I}_{e3,c} = \int_{-\infty}^{\infty} |\hat{F}_c(\omega)|^2 J_n(\beta\omega) \sin(\beta_0\omega)\, d\omega$$

$$= (i\pi/2\omega_0)[-(n-1) J_n(\beta\omega_0) \sin(\beta_0\omega_0) + \beta\omega_0 J_{n-1}(\beta\omega_0) \sin(\beta_0\omega_0)$$

$$- (2\pi - \beta_0\omega_0) J_n(\beta\omega_0) \cos(\beta_0\omega_0)] U(2\pi/\omega_0 - \beta_0 - \beta)$$

$$+ (i\pi/\omega_0)[(n-1) J_n(\beta\omega_0) \sin(\beta_0\omega_0) - \beta\omega_0 J_{n-1}(\beta\omega_0) \sin(\beta_0\omega_0)$$

$$- \beta_0\omega_0 J_n(\beta\omega_0) \cos(\beta_0\omega_0)] U(\beta_0 - \beta)$$

$$+ (i\pi/2\omega_0)[-(n-1) J_n(\beta\omega_0) \sin(\beta_0\omega_0) + \beta\omega_0 J_{n-1}(\beta\omega_0) \sin(\beta_0\omega_0)$$

$$+ (\beta_0\omega_0 - 2\pi) J_n(\beta\omega_0) \cos(\beta_0\omega_0)] U(\beta_0 - 2\pi/\omega_0 - \beta)$$

$$+ (i\pi/2\omega_0)[-(n-1) J_n(\beta\omega_0) \sin(\beta_0\omega_0) + \beta\omega_0 J_{n-1}(\beta\omega_0) \sin(\beta_0\omega_0)$$

$$+ (2\pi + \beta_0\omega_0) J_n(\beta\omega_0) \cos(\beta_0\omega_0)] U(2\pi/\omega_0 + \beta_0 - \beta), \qquad (56a)$$

when n = 0, or even integer

$$\mathcal{I}_{e3,c} = (\pi/2\omega_0)[-(n-1) J_n(\beta\omega_0) \cos(\beta_0\omega_0) + \beta_0\omega_0 J_{n-1}(\beta\omega_0) \cos(\beta_0\omega_0)$$

$$+ (2\pi - \beta_0\omega_0) J_n(\beta\omega_0) \sin(\beta_0\omega_0)] U(2\pi/\omega_0 - \beta_0 - \beta)$$

$$+ (\pi/\omega_0)[-(n-1) J_n(\beta\omega_0) \cos(\beta_0\omega_0) + \beta_0\omega_0 J_{n-1}(\beta\omega_0) \cos(\beta_0\omega_0)$$

$$- \beta_0\omega_0 J_n(\beta\omega_0) \sin(\beta_0\omega_0)] U(\beta_0 - \beta)$$

$$+ (\pi/2\omega_0)[(n-1) J_n(\beta\omega_0) \cos(\beta_0\omega_0) - \beta\omega_0 J_{n-1}(\beta\omega_0) \cos(\beta_0\omega_0)$$

$$- (\beta_0\omega_0 - 2\pi) J_n(\beta\omega_0) \sin(\beta_0\omega_0)] U(\beta_0 - 2\pi/\omega_0 - \beta)$$

$$+ (\pi/2\omega_0)[(n-1) J_n(\beta\omega_0) \cos(\beta_0\omega_0) - \beta\omega_0 J_{n-1}(\beta\omega_0) \cos(\beta_0\omega_0)$$

$$+ (2\pi + \beta\,\omega_0)\, J_n\,(\beta\,\omega_0) \sin(\beta_0\,\omega_0)]\; U\,(2\pi/\omega_0 + \beta_0 - \beta) \qquad (56b)$$

when n = odd integer.

REFERENCES

1. L.C. Martin and W.T. Welford, *Technical Optics-Vol I, Sir Isaac Pitman & Sons, London, pp. 82-88, 1966.*

2. E. Hecht, *Optics* (2nd Edn), Addison-Wesley, Reading, MA, pp. 396-397, 1987.

3. V.M. Ristic, *Principle of Acoustic Devices*, Chapt. 10, New York, Wiley, 1983.

4. S. Silver, *Microwave Antenna Theory and Design*, M.I.T. Rad. Lab. Ser, Vol. 12, McGraw-Hill Book Co., New York, N.Y. pp. 170-172, 196-199, 1949.

5. T.T. Wu, "Electromagnetic Missiles," J. Appl. Phys., Vol. **57**, pp. 2370-2373, 1985.

6. H.M. Shen and T.T. Wu, "The Properties of the Electromagnetic Missile," J. Appl. Phys., Vol. **60**, pp. 4025-4034, 1989.

7. R.W. Ziolkowski, "Localized Transmission of Electromagnetic Energy," Phys. Rev. A. Vol. **39**, pp. 2005-2033, 1989.

8. R.W. Ziolkowski, D. Kent Lews and B.D. Cook, "Evidence of Localized Wave Transmission," Phys. Rev. Letters, Vol. 62, pp. 147-150, 1989.

9. M.K. Hu, "Fresnel Region Field Distribution of Circular Apertune Antennas," IEEE Trans. Antennas Propagat., Vol. AP-34, pp. 344-346, May 1960.

10. G.N. Watson, *A Treatise in the Theory of Bessel Functions*, Cambridge University Press, (2nd Edn), pp. 537-540, 1952.

11. M. Born and E. Wolf, *Principles of Optics* (6th Corrected Edn), Pergaman Press, pp. 435-444, 1988.

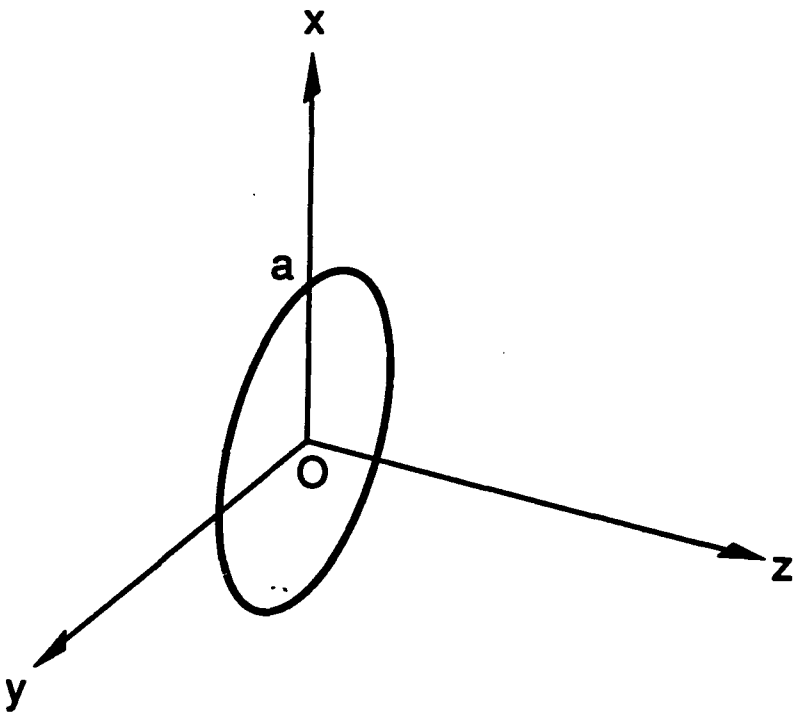

Fig. 1 — A circular disk of radius a = D/2, which is excited by uniform single-cycle sinusoidal currents.

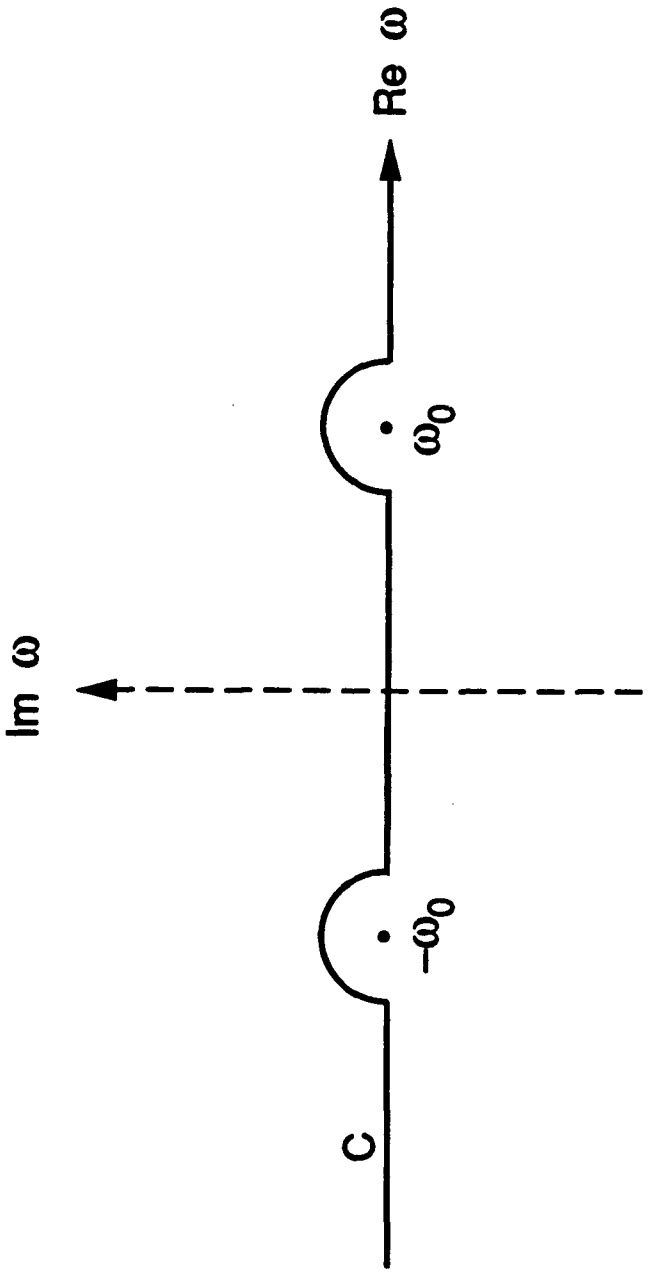

Fig. 2 — Path of integration C in the complex ω-plane

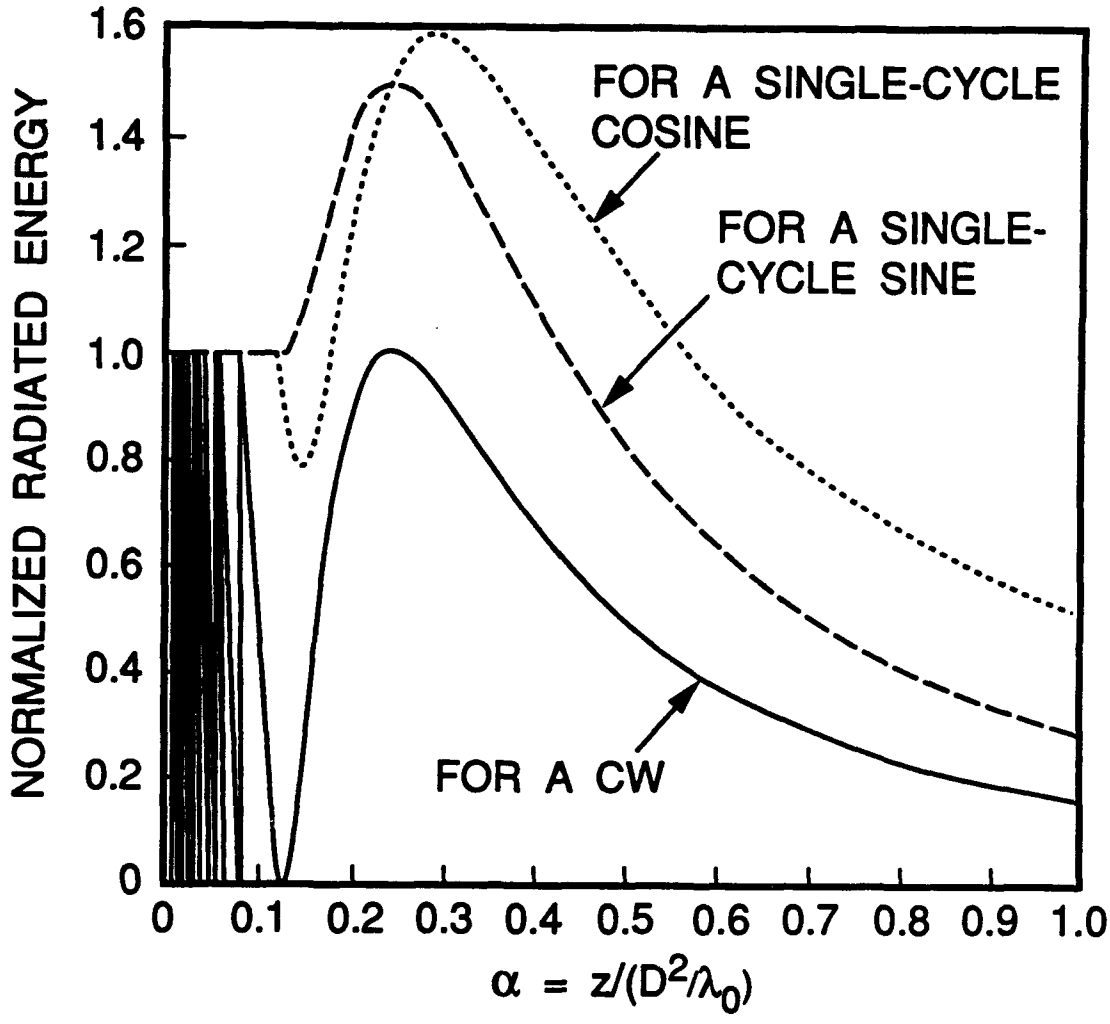

Fig. 3a — Normalized energy densities along the axis of the disk for $\alpha < 1$

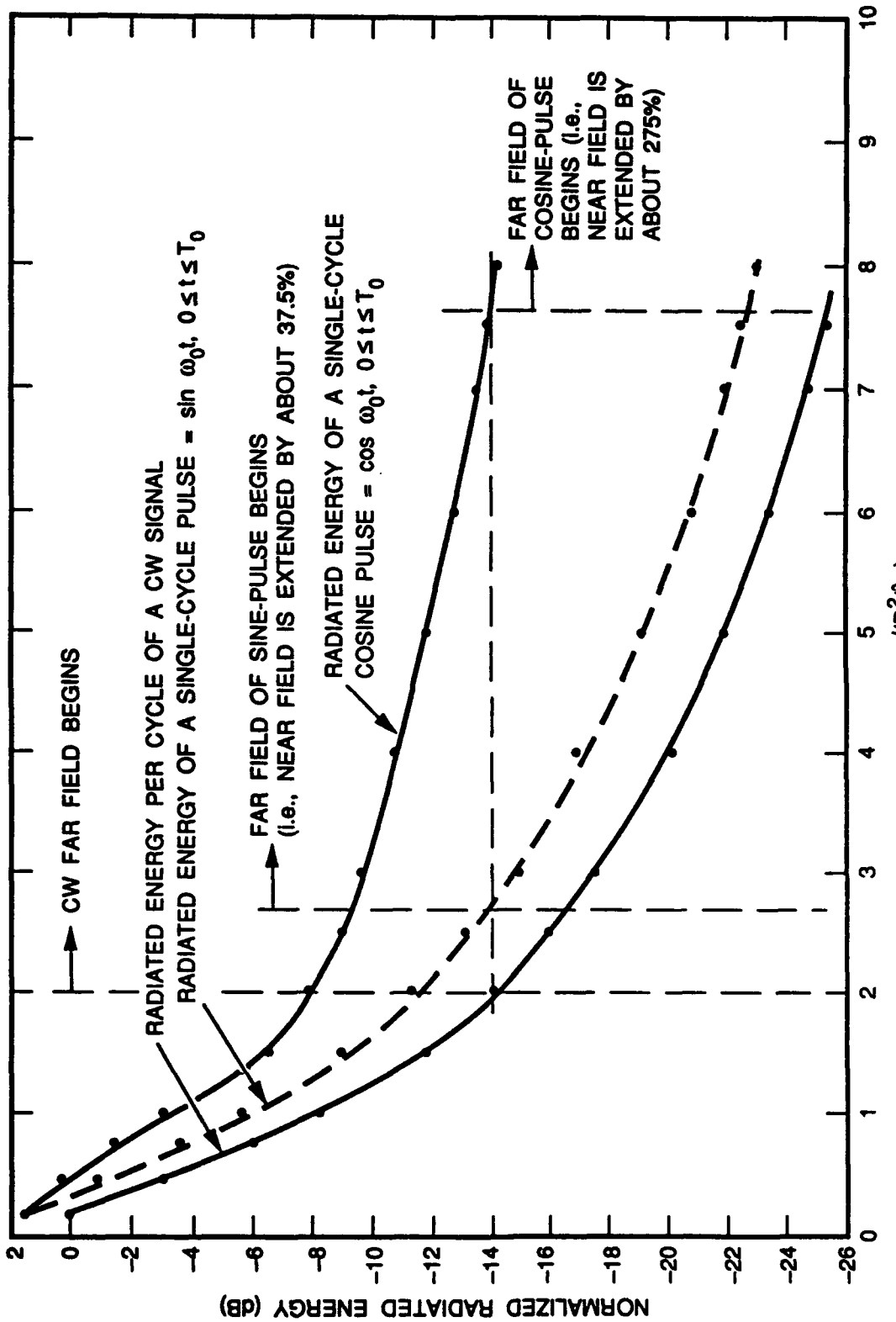

Fig. 3b — Normalized energy densities along the axis of the disk for $\alpha > 1$

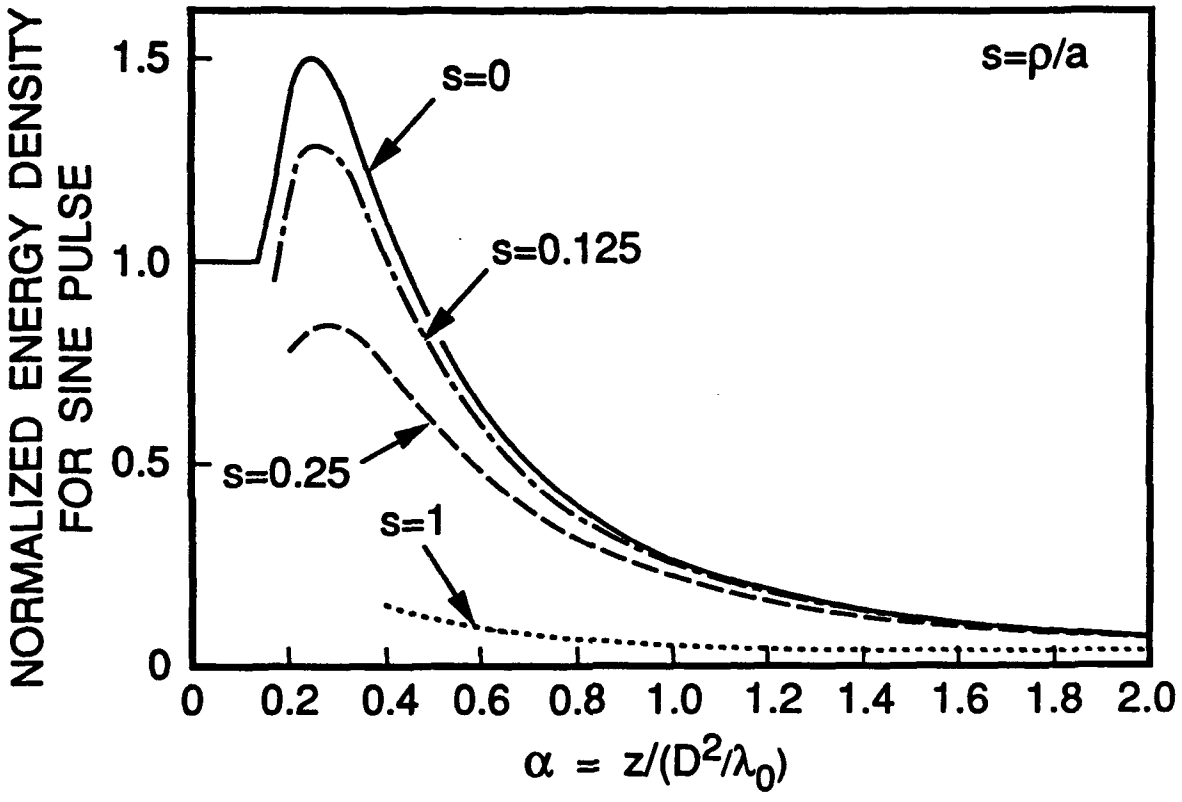

Fig. 4a — Normalized energy densities associated with the single-cycle $\sin\omega_0 t$ for different values of s

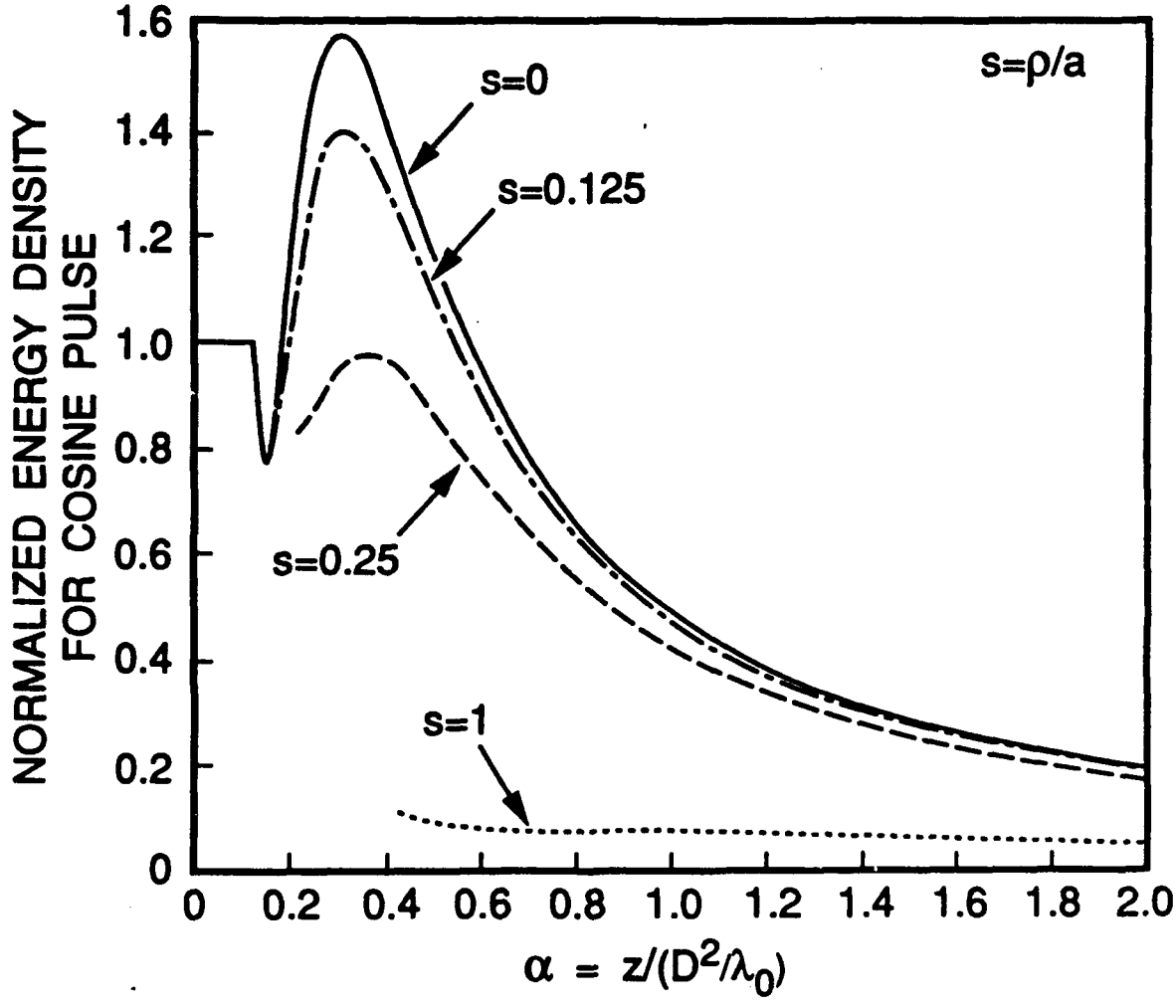

Fig. 4b — Normalized energy densities associated with the single-cycle $\cos\omega_0 t$ for different values of s

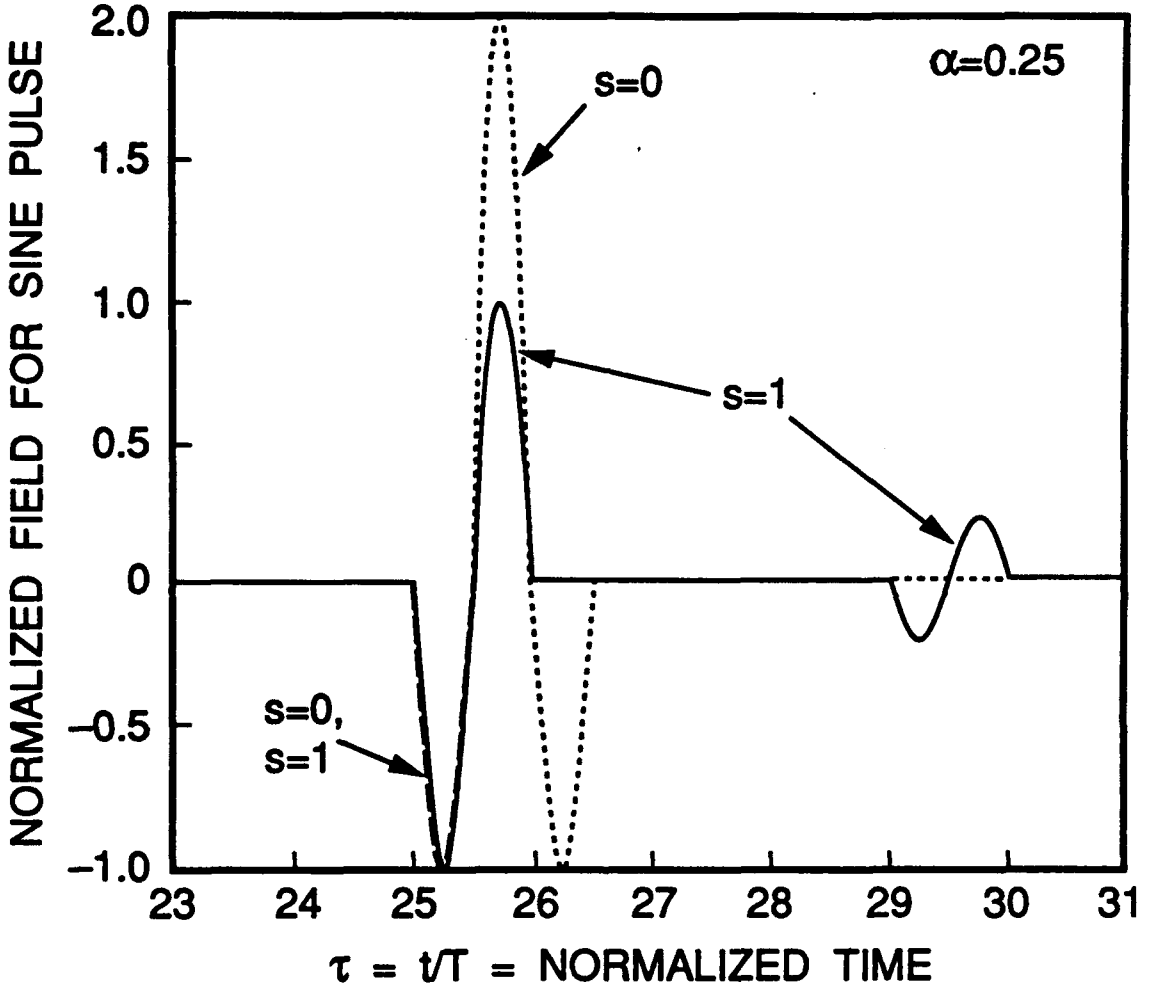

Fig. 5a — Normalized field as a function of τ for $\alpha = 0.25$

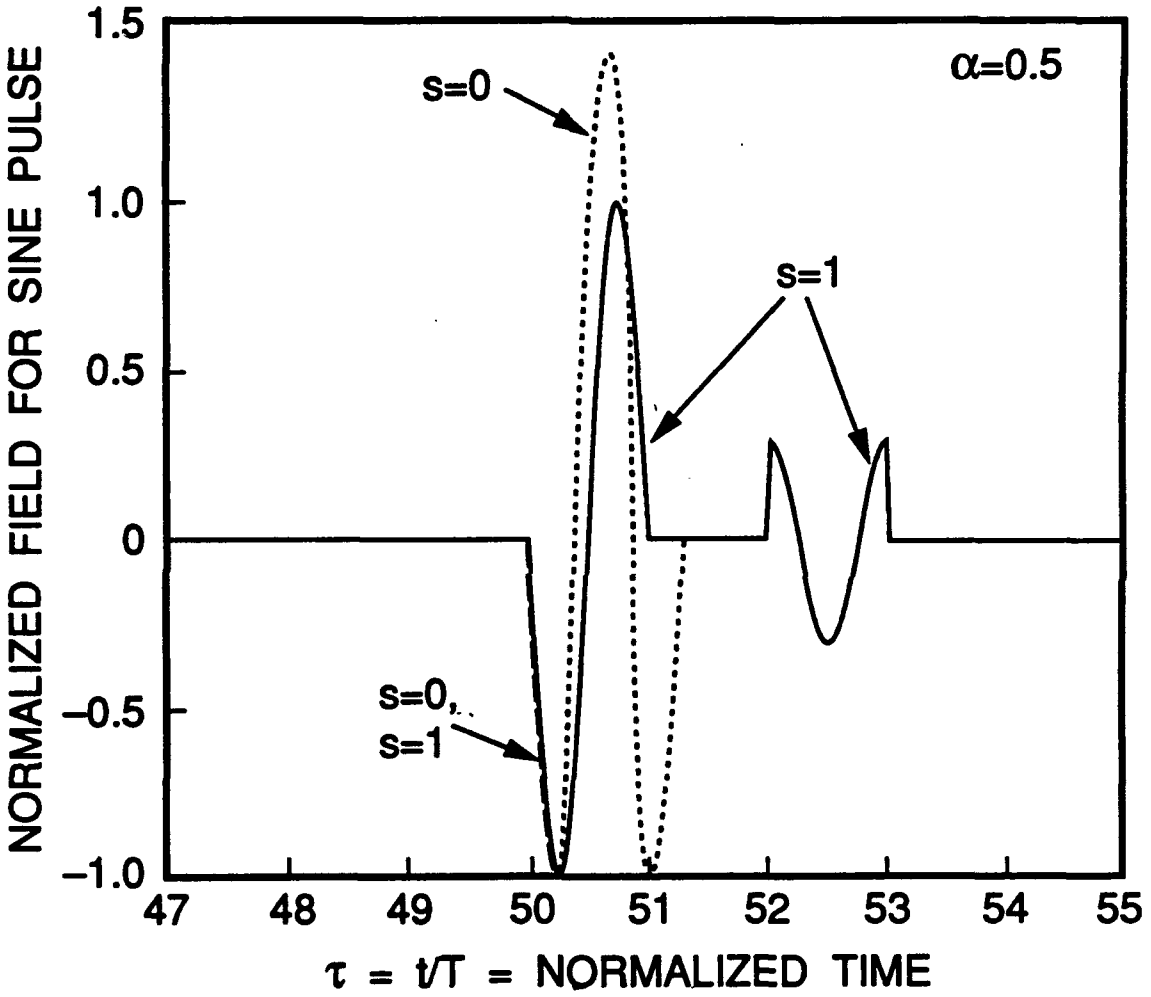

Fig. 5b — Normalized field as a function of τ for $\alpha = 0.5$

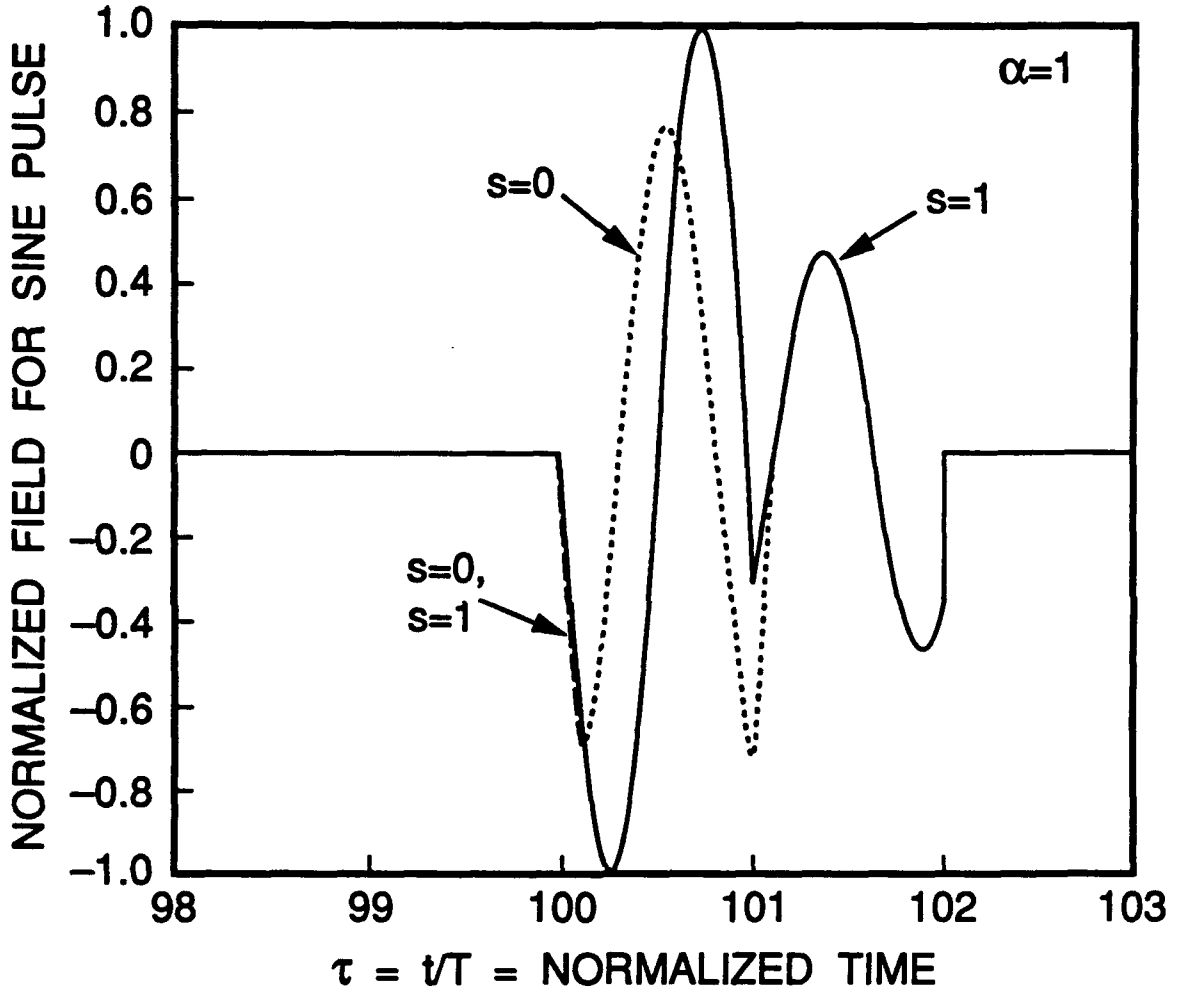

Fig. 5c — Normalized field as a function of τ for $\alpha = 1.0$

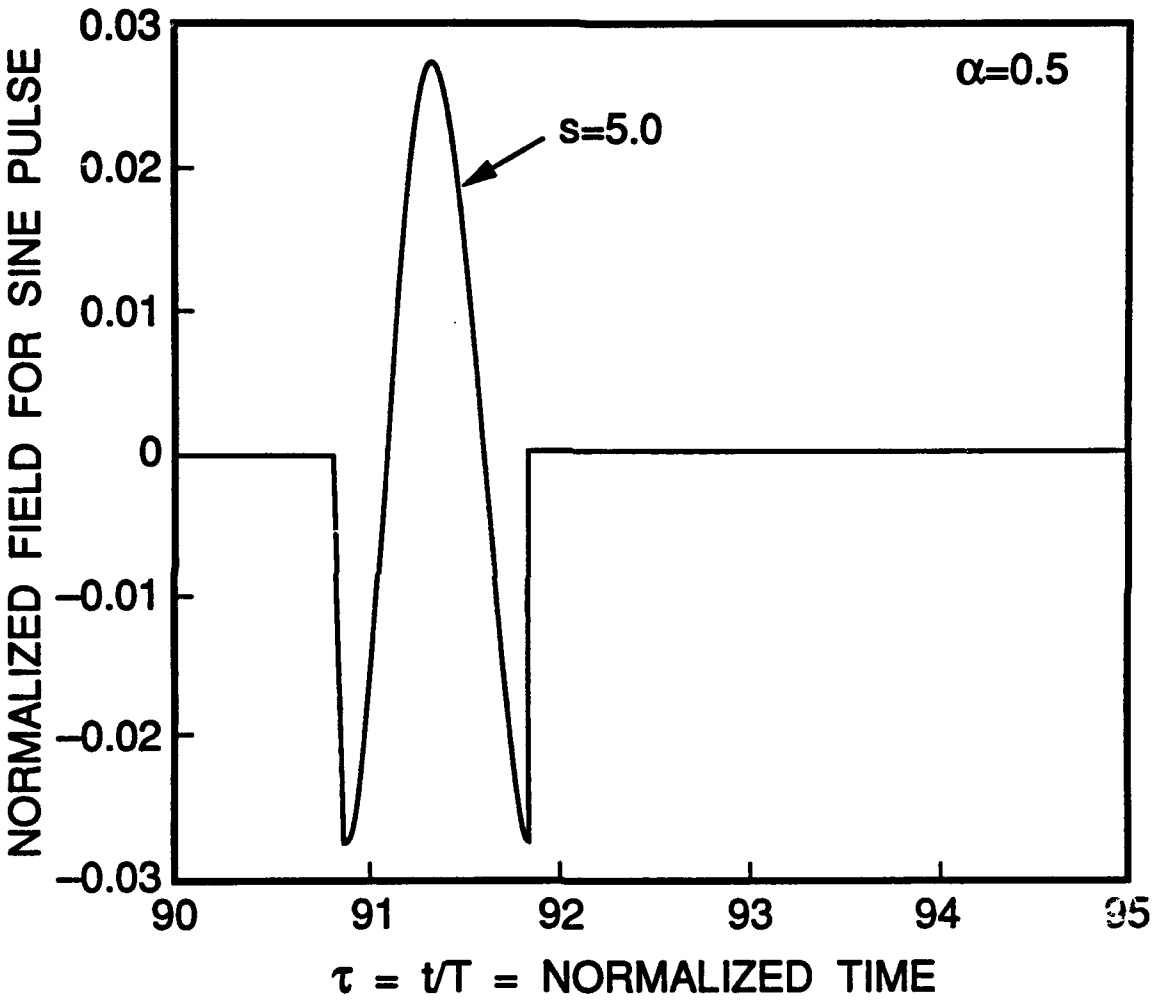

Fig. 5d — Normalized field as a function of τ for $\alpha = 0.5$